

IAEA-TECDOC-974

***Trends and techniques in
neutron beam research
for medium and low flux
research reactors***

*Report of a consultants meeting
held in Mumbai, India, 16–19 March 1996*



INTERNATIONAL ATOMIC ENERGY AGENCY

IAEA

The IAEA does not normally maintain stocks of reports in this series.
However, microfiche copies of these reports can be obtained from

INIS Clearinghouse
International Atomic Energy Agency
Wagramerstrasse 5
P.O. Box 100
A-1400 Vienna, Austria

Orders should be accompanied by prepayment of Austrian Schillings 100,—
in the form of a cheque or in the form of IAEA microfiche service coupons
which may be ordered separately from the INIS Clearinghouse.

The originating Section of this publication in the IAEA was

Physics Section
International Atomic Energy Agency
Wagramerstrasse 5
P.O. Box 100
A-1400 Vienna, Austria

TRENDS AND TECHNIQUES IN NEUTRON BEAM RESEARCH FOR
MEDIUM AND LOW FLUX RESEARCH REACTORS

IAEA, VIENNA, 1997

IAEA-TECDOC-974

ISSN 1011-4289

© IAEA, 1997

Printed by the IAEA in Austria

October 1997

FOREWORD

Neutrons serve as a complementary probe to X rays and other techniques for a wide range of applications. These include studies of diverse properties and material testing and characterization. Neutron beams are also used in some of the most fundamental applications in basic research in condensed matter physics.

Early research using neutron beams focused on standard techniques such as diffraction or inelastic scattering. However, over the past three decades, the techniques have become quite diverse and sophisticated. Notable examples include neutron spin-echo spectroscopy, neutron optics and reflectometry, small angle neutron scattering, etc.

The IAEA is making concerted efforts to promote R&D programmes for neutron beam research to assist the developing Member States in better utilization of their research reactors. A consultants meeting was organized on 16-19 March 1996 to review the current status and deliberate on the future trends in neutron beam based research using low and medium flux research reactors with the flux range of the order of up to 10^{13} - 10^{14} n/cm²/s, particularly in the light of recent advances in electronics and instrumentation.

The participants focused on five specific topics: triple axis spectrometry, neutron depolarization studies, capillary optics, spin-echo spectrometry and small-angle neutron spectrometry. This TECDOC details the highlights of the discussions in the meeting along with the papers presented.

It is hoped that this publication will help improve the utilization of low and medium flux research reactors and the further exploitation of neutron beam techniques in materials science.

The IAEA staff members responsible for this publication were K. Akhtar and V. Dimic of the Division of Physical and Chemical Sciences.

EDITORIAL NOTE

In preparing this publication for press, staff of the IAEA have made up the pages from the original manuscripts as submitted by the authors. The views expressed do not necessarily reflect those of the IAEA, the governments of the nominating Member States or the nominating organizations.

Throughout the text names of Member States are retained as they were when the text was compiled.

The use of particular designations of countries or territories does not imply any judgement by the publisher, the IAEA, as to the legal status of such countries or territories, of their authorities and institutions or of the delimitation of their boundaries.

The mention of names of specific companies or products (whether or not indicated as registered) does not imply any intention to infringe proprietary rights, nor should it be construed as an endorsement or recommendation on the part of the IAEA.

CONTENTS

1. INTRODUCTION.....	7
2. HIGHLIGHTS OF THE TOPICS DISCUSSED	8
2.1. Triple axis spectrometry.....	9
2.1.1. Beam tubes and moderators for triple axis spectrometry	9
2.2. Neutron depolarization studies.....	9
2.3. Small-angle neutron scattering.....	10
2.3.1. Types of instruments	10
2.3.2. General considerations	11
2.4. Neutron spin-echo spectroscopy (NSE).....	11
2.5. Polycapillary neutron lenses.....	12
3. CONCLUSION AND RECOMMENDATIONS.....	14
REFERENCES.....	16
ANNEX: PAPERS PRESENTED AT THE MEETING	
Triple axis spectrometers	19
<i>K.N. Clausen</i>	
Neutron depolarisation in magnetic materials	35
<i>M.T. Rekveldt</i>	
Small angle neutron scattering.....	43
<i>B.A. Dasannacharya, P.S. Goyal</i>	
Neutron spin echo.....	55
<i>B. Farago</i>	
Polycapillary neutron lenses.....	63
<i>D.F.R. Mildner</i>	
LIST OF PARTICIPANTS	71

1. INTRODUCTION

During the last nearly 50 years since the first reactor 'pile' was established at Chicago, a number of research reactors have been built the world over. At present as many as about 300 research reactors of different power ratings are under operation or in operable condition. They are being used, in addition to neutron beam research in condensed matter, for a variety of applications such as isotope production, neutron activation analysis, studies connected with nuclear power reactor fuels, components and structural materials. The neutron beam based research at research reactors is largely centered around crystal spectrometers whereas at the pulsed neutron sources the time-of-flight (TOF) method is used. During the past 30 years or so, a variety of neutron beam tailoring techniques have been developed. These are based on hot and cold neutron moderators, neutron guides, multi-detector systems and special monochromators. Neutron diffraction and triple axis neutron spectrometry developed by Shull and Brockhouse respectively in the late forties and fifties received recognition by the award of the Nobel Prize in Physics to them in 1994. The original concepts of diffraction and triple axis spectrometry they developed are still in vogue and form the backbone for further developments using low and medium flux reactors. Polarized neutron diffraction and analysis techniques, back-scattering high resolution inelastic spectroscopy, correlation techniques, neutron interferometry, neutron spin-echo spectroscopy, three dimensional depolarization analysis and small-angle neutron scattering are some of the later developments which have flourished in many research reactor centres. It is noteworthy that experiments on a variety of materials carried out at low and medium flux reactors at the Atominstitut (Austria), IRI (Netherlands), RISØ (Denmark), MURR (Japan), etc. have been in the forefront of early developments of some of these techniques.

The advances and results obtained during the 1960s are summarized in "Instrumentation for Neutron Inelastic Scattering Research" published by the IAEA in 1970 just before the commissioning of the High Flux Reactor at ILL in Grenoble. Though this publication refers to Inelastic Scattering in the title of the document, it is in reality a compendium of papers presented and discussions held in the Panel of Experts' Meeting organized by the IAEA in Vienna in 1969. There have been many other publications related to neutron inelastic scattering arising out of various IAEA symposia and conferences which also detail many developments in the techniques and instrumentation in this field. These are serving as useful reference documents for the growth of research in this area of utilization of research reactors.

There has been a slowing down in the construction of new research reactors in North America and in Europe during the past decade, principally because of concerns following the Chernobyl accident, and the closure of several reactors in the western world. However, a number of new research reactors have been established during this period in the developing countries, especially in Asia. In addition many European reactors have been or are being upgraded. Avenues for neutron beam research in these and other functional reactors have been a topic of intense discussion at different times. There is a need to review and highlight significant developments in neutron beam research in the light of experience gathered so far, particularly during the last two decades.

The technological advances in miniaturization of electronics, the advent of personal computers, new detectors, supermirrors, etc., are resulting in a large increase in the throughput of data acquisition from small samples, a reduction in the size of instruments, capabilities for real time experiments, on-line data analysis, etc. It is likely that advances in micro-strip and image plate detectors and the development of polycapillary fibres during this decade will result in compact neutron spectrometers. Such developments are bound to enhance usage of low and

medium flux research reactors for a variety of new materials science studies. Even though the neutron flux levels of reactors has not significantly changed during the last two decades, the actual utilization of neutrons is far more effective now because of the overall developments in instrumentation, neutron beam tailoring, neutron transportation, spectrometer design and so on. This publication is intended to record the highlights of the outcome of discussions which took place among a small group of experts on a set of specific topics at a meeting held at the Bhabha Atomic Research Centre, Trombay during March 16-19, 1996.

The following five specific topics were discussed:

1. Triple axis spectrometry
2. Depolarization studies
3. Neutron optics and capillary lenses
4. Spin-echo spectrometry
5. Small-angle neutron scattering.

2. HIGHLIGHTS OF THE TOPICS DISCUSSED

2.1. TRIPLE AXIS SPECTROMETRY

Triple axis spectrometer (TAS) is a versatile and powerful tool for probing the dynamics of single crystals. It has provided key information for the understanding of magnetism, superconductivity, phase-transitions, ion diffusion, lattice dynamics, etc.

The excitations of crystals are in general either delta functions or narrow peaks centered around dispersion surfaces. That is, information is concentrated in a very limited fraction of \underline{Q} , ω space (\underline{Q} is the wavevector transfer and ω is the energy transfer in the scattering process). Selectively focusing on a series of single points in this 4-dimensional space has proven to be an efficient method, because each point has a large information content. Furthermore, measurements based on a series of point by point scans are simple to control and easy to analyze. Hence the large success of the triple axis spectrometer. Improvements on triple axis spectrometers to extend beyond point by point scan will be useful in practice only if it allows several points, approximately a resolution width apart, to be recorded at the same time, i.e., to measure a complete or a part of a standard scan with one setting of the spectrometer. A multielement analyzer and an area-sensitive detector, or a row of many single detectors could be possible solutions for such an improvement. The same arrangement would also allow a more efficient mapping of extended regions in (\underline{Q} , ω) space from systems where the scattering function is a smoothly varying function of \underline{Q} and ω . (e.g. powders, disordered systems, spin fluctuations in high-temperature superconductors, broad quasielastic scattering).

A triple axis spectrometer is also a versatile and flexible instrument which can be used in several different modes and for testing of new instrumental concepts. In most small and medium flux reactors, triple axis spectrometer is often also used as a diffractometer (for very weak scatterers whereas the signal-to-background is critical), a diffuse scattering spectrometer (especially when fitted with an area detector), a reflectometer or to test reflection or small-angle neutron scattering (SANS) concepts. In general, a triple axis spectrometer is one of the best instruments suited for training in spectrometry.

As a pragmatic approach, a triple axis spectrometer should be built in a modular fashion. To start with, a simple version could be built, and later the different axes, monochromator-analyser systems, guide optics or detector systems may be upgraded as improved components or funds become available. Right from the initial concept it is, however, very important to carefully consider the shielding requirements for maximum efficiency, and choose an overall design, which is amenable for changes or upgrades.

While designing the triple axis spectrometer, provisions should be made for the use of several methods for focusing optics. Monochromators focusing in the vertical plane is a minimum requirement. Provisions should be made for use of polarizing filter, i.e., magnetic materials should be avoided in and just around the beam channel. Ultra-high resolution measurements using the spin-echo technique as an add-on to a triple axis spectrometer are not recommended at a low or medium flux reactor. The flux level will be too low to justify the extra investment.

Many new developments are pushing triple axis spectroscopy into new areas of (Q, ω) space. Increased intensity and effectiveness is allowing smaller samples and weak cross sections to be investigated. Triple axis spectroscopy at steady state sources is an open and lively field where young scientists with new ideas can make substantial contributions, and the triple axis spectrometer will continue to be the instrument of choice for many experiments, especially at good reliable reactors with cold sources.

2.1.1. Beam tubes and moderators for triple axis spectrometry

The triple axis spectrometer is most powerful for cold and thermal neutrons. If a cold source is planned, then hydrogen or deuterium moderated cold sources are to be preferred. Solid D_2O ice has been tried at NIST in USA and was abandoned because of poor performance relative to the liquid hydrogen moderator; methane tends to polymerize in the radiation field. From an intuitive licensing point of view the latter two sources might sound more interesting, but in reality the hydrogen sources are safer, better and more reliable. A hot source for a crystal monochromator triple axis spectrometer can be recommended if only careful measures are taken to have a very clean beam. Any material exposed to short wavelength neutrons will scatter neutrons, which can later cause spurious peaks in the detector. Pulsed sources (TOF technique) will in general are preferred for neutron scattering with high energy and momentum transfers.

TAS beam tubes should avoid direct view of the reactor core for background reasons. Tangential or through tubes should be used. A cold neutron high-resolution TAS should preferentially be located at a guide in the guide hall, whereas for cold high-intensity, thermal or hot neutron TAS should be as close to the reactor core as possible (i.e. in the reactor hall). For the cold and thermal neutron TAS short supermirror guides in the outer part of the beam tube will be advantageous.

2.2. NEUTRON DEPOLARIZATION STUDIES

From the discussions on neutron depolarization studies, it is evident that neutron depolarization is a powerful technique to study the magnetic correlation length in a variety of magnetic systems which have importance both from basic and applied research point of view. The advantage of such studies is that it does not require very high incident neutron flux. Depolarization measurements can be carried out even in a small reactor with 100 kW power and with a core flux of the order of 10^{12} n/cm²/s. The fast determination of a magnetic correlation

length in a depolarization experiment makes this technique very suitable to study such a parameter as a function of external parameters as magnetic field or others. Though the experiments can be carried out using single crystals as polarizes/analyzer, it is recommended to use a graphite monochromator with supermirrors as polarizes/analyzer in order to enhance the intensity. It may be noted that at present polarizing supermirrors are available which work even at a wavelength of 0.16 nm, angular divergence of 7 mrad and with very high polarization efficiency of 0.98. At a wavelength of 0.16 nm the overall transmission of the right spin can be 50% which is close to the theoretically achievable value.

In order to extract maximum information from depolarization studies it is advisable to perform three dimensional measurements instead of one dimensional. From three dimensional studies, one can get information about the mean magnetic correlation length, mean magnetization and mean direction cosine of local magnetization. It has been proved that the wavelength dependence studies can give additional information such as the distribution of correlation lengths. It may be added that neutron depolarization will continue to occupy a special position in investigations of magnetic materials since they provide unique information under various circumstances.

2.3. SMALL-ANGLE NEUTRON SCATTERING

Small-angle neutron scattering (SANS) has become one of the most popular neutron beam instruments during recent times for the twin reasons of its being both a basic research technique as well as a tool in the hands of applied scientists. SANS experiments give structural information on length scale from ~ 10 - 10000 \AA , depending on the type of spectrometer utilized. This covers a length scale of particular interest to a number of applied problems relating to polymers, surfactants, metallurgical precipitates, ceramics, biological molecules, etc. Depending on the length scale, L , of interest it is necessary to use an instrument which covers the corresponding wave-vector transfer range, Q , approximately $\sim 2\pi/L$. Thus, the Q coverage could extend from 10^{-5} to 10^{-1} \AA^{-1} . It is not possible to cover this range with a single instrument and different machines have therefore been designed.

2.3.1. Types of instruments

$Q \sim 10^{-5} - 10^{-3} \text{ \AA}^{-1}$: This Q range can only be covered by using double crystal diffractometers. In this, one uses two perfect Si crystals aligned parallel to each other. Insertion of a sample between the two crystals broadens the beam falling on the second crystal. This broadening is measured by rocking the second crystal and the measured intensity as a function of angle is related to the structural characteristics of the material. Inherently, this is a very simple device and can be used even with very modest flux reactors. Introduction of channel-cut Si crystals in place of ordinary ones can help reduce the diffuse wings and increase the Q range. Bent crystals have also been used to increase the Q_{max} . These experiments can be performed on a good standard triple axis machine.

$Q \sim 10^{-3}$ to $5 \times 10^{-1} \text{ \AA}^{-1}$: This Q range is covered in a conventional SANS spectrometer which was developed first at Juelich. In this machine, a well collimated and a moderately monochromatic beam ($\delta\lambda/\lambda \sim 0.1$ to 0.2) is extracted from the reactor by means of a monochromator (usually a velocity selector) and the collimating apertures. The sample scatters neutrons through small angles and the intensity as a function of scattering angle is detected and recorded by neutron detectors and data acquisition instrumentation down stream. The choice of flight paths and the incident wavelength depends on the Q range and the resolution.

SANS instruments covering a Q range $0.02-0.5 \text{ \AA}^{-1}$ can be built easily. SANS instruments at Cirrus reactor, Trombay, for example, uses a BeO filtered beam ($\lambda = 5.2 \text{ \AA}$) and primary and secondary flight paths of $L_1 = 2.5 \text{ m}$ and $L_2 = 1.8 \text{ m}$ respectively. This spectrometer provides a Q range of $0.02 - 0.5 \text{ \AA}^{-1}$ with a sample size of $1.0 \times 1.5 \text{ cm}$. However, to obtain lower Q values, one has to tighten the collimations and there should be a provision to use larger incident wavelength. In high resolution instruments, flight paths up to $L_1 = L_2 \sim 40 \text{ m}$ and λ up to 10 \AA have been used. To obtain higher counting rates, these instruments employ two dimensional position-sensitive detectors and cold neutron sources. The mechanical velocity selector is the most commonly used monochromator for these instruments. It is, however, possible to use pairs of double crystal monochromators and obtain $\delta\lambda/\lambda$ in range of .05 to 0.10. The double monochromator works at a fixed wavelength but has an advantage that it takes the monochromatic beam away from the direct beam and thus has less contribution from fast neutrons or γ rays. The use of filters or filters followed by mirrors can also be used profitably for the purpose of a monochromator.

2.3.2. General considerations

It is often seen that SANS instruments are installed on cold source beam lines. This is highly desirable but also expensive. There is a large class of experiments however, which can be easily done without a cold source (such is the case at ORNL). Secondly, 2D position-sensitive detectors also are highly recommended but extremely expensive, particularly since they are often of very large dimensions. This is because in a gas detector the charge cloud cannot be reduced in size below a few mm, and the neutron beams are necessarily large ($\sim 1 \text{ cm}^2$) in order to increase the counting rate in the detector. With all these considerations, there is a need to think in terms of methods which would reduce costs.

Photographic methods (using image plates) and 'suitably' focused beams should be considered as distinct possibilities. It is also well known that $\delta\lambda/\lambda$ can be allowed to be very large. Beam tailoring using filters can be quite promising as experienced at CIRUS.

2.4. NEUTRON SPIN-ECHO SPECTROSCOPY (NSE)

NSE is a special technique which decouples beam monochromatisation from energy resolution. The first NSE spectrometer (IN11) at the ILL Grenoble, for example, uses 18% FWHM beam monochromatisation while achieving as low as 2 neV energy resolution. This makes it suitable to perform high resolution quasielastic experiments even at medium flux reactors. There are however a few points where particular attention should be paid.

NSE needs a polarized beam and severe intensity losses can result from the polarizer-analyzer pair. Especially if the polarizing supermirrors are in reflection mode, they might severely increase the beam divergence. If typically the polarizer-sample distance is in the order of 1-3 m to accommodate the precession field coils, this might substantially reduce the neutron flux on the sample. With the recent developments in polarizing supermirrors (ILL, HMI, PSI) the best choice seems to be the transmission polariser arrangement. This provides also a flexible way to change back and forth the wavelength during the experiment to best match the resolution with the available intensity without physically changing the instrument configuration. On the analyzer side, the requirements are more relaxed as the detector is normally very close to the analyzer.

The use of a cold neutron beam is really essential. Firstly because the resolution improves rapidly with the wavelength, secondly because the efficient production of a polarized beam is much easier at longer wavelength (the critical angles increase with wavelength).

The resolution is also proportional to the field integral. However a two fold increase in the instrument length to double the resolution will result in a 16 fold count rate decrease in the detector while the same can be achieved by choosing $\sqrt[3]{2} = 1.26$ times longer wave length. Consequently a shorter instrument is advantageous. Given the necessary place constraint from flippers, etc., the lower limit is around 1 m length precession coils.

The method is inherently sensitive to external magnetic fields, so attention should be paid to using only non magnetic materials for the mechanical construction and in the immediate environment.

Whatever magnetic field design is chosen (solenoids like IN11 at the ILL or wide angle magnets at the HMI spin echo and IN11C at ILL) all configurations have inherently inhomogeneous field integral because of the Maxwell law $\nabla B = 0$. On the other hand, many types of beam correction coils are able to correct this nearly perfectly. However, the ultimate resolution one can reach is not yet known. On the other hand irregularities in the precession coil winding cannot be easily corrected and might become the real limitation.

For neutron spin-echo which measures up to 10^{-5} relative energy transfer of the incoming neutrons, the mechanical stability of the instrument (flipper fixation, thermal expansion of the coils on current heating, etc.) can be important.

For a spin-echo instrument, around 10 current stabilized power supplies must be set to well defined values. Some of them drive the equivalent coils on both sides of the spectrometer (precession coils, Fresnel's correction coils) and slow drifts in the current are not harmful but ripples (e.g. 50 Hz) can destroy the echo. Some of the current supplies, e.g. those for the symmetry coil which allow the exact matching of the field integral must be stable to 10^{-4} to 10^{-5} level.

If the wide-angle magnets mentioned above perform as predicted, they represent an alternative option (as in IN11C) for high Q studies with some sacrifice in best resolution (estimated to 1/2 to 1/3) but with an increased count rate of 10-20 fold higher as more Q values are measured simultaneously. Of course this represents an advantage only if all Q values are of interest for the physical problem studied.

Zero field NSE is an interesting approach to have a compact instrument but still perform adequately especially for high-angle studies. The high frequency requirement should be less of a problem with today's electronics, but the slim high static field coils are not easy to make. The method is just reaching its first phase (beyond demonstration stage). The results and eventual problems should be followed on.

2.5. POLYCAPILLARY NEUTRON LENSES

Neutron guides are used to transport beams to areas of low background at many reactors around the world, particularly those with cold neutron sources. This is done using the principle of multiple mirror reflection at small grazing angles from smooth surfaces (usually nickel, ^{58}Ni or supermirror coatings on glass). This same principle can be used for transporting neutrons

through tiny hollow glass capillaries with transverse dimensions $\sim 10 \mu\text{m}$. The great advantage of these miniature neutron guides is that they can enable beam of long wavelength ($\lambda \sim 4\text{\AA}$) neutrons to be transmitted reasonably efficiently through a radius of curvature as small as a fraction of 1 m. A large collection of these capillaries can be used to form a neutron lens to bend the trajectories such that the incident neutron beam can be focused. While this is more efficiently performed for cold neutron beams, thermal neutron beams can also be bent.

The idea of using tiny channels for transporting and guiding neutrons is relatively new, and this may be able to improve the capabilities of certain neutron techniques. It is important to know that the concept depends on accurate alignment. A typical lens contains over a thousand glass fibers of diameter $\sim 0.5 \text{ mm}$, each of which contains over a thousand hollow capillaries of diameter $\sim 10 \mu\text{m}$. At the entrance of the lens all the fibers are held parallel to each other and to the axis of the beam. At the exit of the lens all the fibers point exactly to the same point beyond the lens. Consequently over a million channels can accept the incident neutron beam and transmit the neutrons to the focus.

In describing both the gain and transmission efficiency of a given lens, it is most important to state the conditions of the incident beam. Both the wavelength and the divergence of the beam incident on the entrance of the lens affect the stated values of both parameters. The various features of polycapillary lenses may be summarized as follows:

- (i) The gain in neutron current density at the focus (1) is dependent on the area reduction, that is, the ratio of the entrance area of the lens and the focal spot size. This means that the gain is determined by the open fraction of the individual fibers, the packing density of these fibers at the entrance of the lens, and the number of fibers, though the outer fibers which curve the most have reduced transmission for short wavelengths. The transmission (2), and therefore the gain, also depends on the ratio of the critical angle of the capillaries and the divergence of the incident beam;
- (ii) The transmission efficiency depends on the glass composition and the surface smoothness, as well as on the internal capillary diameter and the bending radius of the channels. For optimum transmission, the design of a focusing lens using polycapillary fiber optics must take into account the length of the fibers, the number of fibers, and the bending radius of the outer fibers;
- (iii) The focal length of the polycapillary lens depends on its design, but the optimum (3) is determined by the fiber diameter and the critical angle averaged over the spectrum of neutrons transmitted by the lens. In fact, the better transmission characteristics for longer wavelengths gives rise to a shift in the spectrum transmitted through the lens (4);
- (iv) The composition determines the critical angle per unit wavelength, and for most silicate glasses is about $1.1 \text{ mrad } \text{\AA}^{-1}$. It can only be increased if the internal surface can be coated, with nickel for example;
- (v) The number of reflections (5) that a trajectory makes in its passage through the channel depends on the length and diameter of the channel. 4 \AA neutrons make about 40 reflections in their passage through a glass channel of length 100 mm and diameter of $10 \mu\text{m}$, and more if the channel is curved. Hence the inner surface of the fiber must have excellent reflectivity characteristics for reasonable transmission;

- (vi) The depth of focus (1) depends on the convergence angle of the outer fibers, and only mildly on the radius of the fibers and the critical angle (which determines the exit beam divergence), whereas the size of the focal spot is resolved by these latter parameters.

Some of these considerations are summarized in Table I.

TABLE I. PARAMETERS TO BE CONSIDERED FOR A NEUTRON LENS

Gain of lens at focus	$G \sim (\theta_c/\theta_d)^2 N R^2 f_F [R^2 + (L_F\theta_c)^2]^{-1}$
Optimization for focal length	$L_F \sim R/\theta_c$
Variance of spatial distribution	$\sigma^2(L) \sim 1/2 [L_F - L]^2 \tan^2\Omega + R^2 + (L\theta_c)^2$
Number of reflections	$N_R \sim \theta_c l/d$

l is the length of the fiber, R is the radius of the fiber, d is the diameter of a channel, f_F is the open fraction of a fiber, θ_c is the critical angle for the glass averaged over the spectrum of transmitted neutrons, θ_d is the divergence of the beam incident on the lens, N is the number of fibers in the lens, Ω is the convergence angle of the focused beam, and L is the distance from the end of the lens.

3. CONCLUSIONS AND RECOMMENDATIONS

1. A modular well designed and flexible triple axis spectrometer should be an instrument of choice at any research reactor. This is an instrument which can be used for inelastic scattering, reflectometry, SANS, diffuse scattering and many other test concepts which cannot be done on a diffractometer. Concepts described above (focusing elements, supermirrors, PSD, multianalysis, etc.) should be incorporated gradually and carefully to improve throughput without unduly sacrificing resolution, but the designer should consider these aspects right from the beginning. Good shielding should be given special attention.
2. Neutrons continue to occupy a special position in the study of magnetic materials. Neutron depolarization investigations are particularly suited to lower flux reactors. Use of supermirrors with PG monochromators could improve flux at the sample considerably and are recommended. Three dimensional measurements are advisable. The possibility of wavelength dependent studies should be kept in mind since they give additional information.
3. Like depolarization studies, small-angle neutron scattering (SANS) yields essential information for basic science and applications, so it is of great interest in almost all neutron scattering centres. Sophisticated and large SANS instruments of the conventional design can be very expensive and quite difficult to maintain (especially if it is with a 2D detector). However, it is possible to design simple and inexpensive instruments if the demand of Q_{min} is relaxed to some extent, e.g., to nearly 0.02 \AA^{-1} . The role of filtered beams, (as compared with velocity selectors) which can be cheap and trouble free, needs careful examination, especially as a start-up programme. Perfect crystal and image plate based instruments have interesting possibilities for the future. 1-D detectors are comparatively easier to maintain and can be gradually built up to give 2D information.

4. Spin-echo spectroscopy, since it decouples energy and momentum resolution, in principle, can be used at medium flux reactors. However, polarization requirements take a heavy toll of the intensity. Supermirrors and wide-angle magnets have a special role in this context. NSE spectroscopy requires cold neutrons for reasons described earlier. It also requires precision and stable instrumentation of power supplies, coils, etc. In summary, NSE spectroscopy can be done at medium flux reactors if latest concepts are incorporated, but very careful planning is required.
5. The technology for focusing a beam of cold neutrons onto a small spot using a polycapillary lens has been developed recently in order to achieve an increased neutron current density on the sample. This is best used for absorption measurements, and has been applied in chemical analysis to enhance the sensitivity of the measurements and to improve the detection limits. This allows for the possibility of two or three dimensional composition mapping. Such development will thereby enhance the measurement capabilities of analytical techniques using neutron absorption such as prompt gamma activation analysis and neutron depth profiling. In view of the many applications in chemistry and condensed matter, the increased use of focusing capillaries may result in the more economic utilization of reactor beams. Other scientific areas will benefit as the technique becomes more developed.
6. The discussions which took place on each technique clearly brought out the extremely live nature of the growth of neutron based sciences even at medium flux (10^{13} - 10^{14} n/cm²/sec) reactors. This has resulted entirely from new developments in techniques, instrumentation and software for the utilization of the available neutrons. It is often possible today to do experiments with an order of magnitude (or more) greater efficiency as compared to, say, twenty years ago with the same reactor. Apart from diffractometry which was not discussed for obvious reasons, triple axis spectrometry, SANS and depolarization measurements are all being pursued at many medium flux reactors. The questions of cost versus output, local interest, and available expertise must always be taken into account when deciding the nature of the required facilities. However, it is often possible to improve the throughputs considerably by sacrificing resolution or range of measurements judiciously. Costs can also be reduced if a careful combination of neutronic elements coupled with good software is utilized. NSE is a more specialized area and established in only a few laboratories. Capillary optics is in its infancy and expected to grow rapidly as a useful tool in activation analysis and scanning radiography.

REFERENCES

- [1] MILDNER, D.F.R., CHEN, H., *J. Appl. Cryst.* **27** (1994) 943-949.
- [2] MILDNER, D.F.R., CHEN, H., *J. Appl. Cryst.* **27** (1994) 316-325.
- [3] MILDNER, D.F.R., *J. Appl. Cryst.* **26** (1993) 721-727.
- [4] MILDNER, D.F.R., CHEN, H., DOWNING, R.G., SHAROV, V.A., XIAO, Q.F., *Acta Physica Hungarica* **75** (1994) 177-183.
- [5] MILDNER, D.F.R., SHAROV, V.A., CHEN, H., *J. Appl. Cryst.* **28** (1995) 69-77.

Annex

PAPERS PRESENTED AT THE MEETING

**NEXT PAGE(S)
left BLANK**



TRIPLE AXIS SPECTROMETERS

K.N. CLAUSEN

Risø National Laboratory,
Roskilde, Denmark

Abstract

Conventional triple-axis neutron spectroscopy was developed by Brockhouse over thirty years ago¹ and remains today a versatile and powerful tool for probing the dynamics of condensed matter. The original design of the triple axis spectrometer is technically simple and probes momentum and energy space on a point-by-point basis. This ability to systematically probe the scattering function in a way which only requires a few angles to be moved under computer control and where the observed data in general can be analysed using a pencil and graph paper or a simple fitting routine, has been essential for the success of the method.

These constraints were quite reasonable at the time the technique was developed. Advances in computer based data acquisition, neutron beam optics, and position sensitive area detectors have been gradually implemented on many triple axis spectrometer spectrometers, but the full potential of this has not been fully exploited yet. Further improvement in terms of efficiency (beyond point by point inspection) and increased sensitivity (use of focusing optics whenever the problem allows it) could easily be up to a factor of 10-20 over present instruments for many problems at a cost which is negligible compared to that of increasing the flux of the source. The real cost will be in complexity - finding the optimal set-up for a given scan and interpreting the data as they are taken. On-line transformation of the data for an appropriate display in Q , ω space and analysis tools will be equally important for this task, and the success of these new ideas will crucially depend on how well we solve these problems.

Introduction

Over the years many individual components have been modified leading to improvements in intensity, resolution, signal/noise, automation, and analysis. Cold, thermal and hot moderators have been installed at many reactors and triple axis spectrometers have been specialised in the same three varieties - each type optimised for its corresponding spectrum.

The development of neutron guides has allowed cold high resolution triple axis work to move into the less confined spatial surroundings and the lower background of a neutron guide hall.

The crystals used to produce the monochromatic beam have improved dramatically. Pyrolytic graphite with its high reflectivity² provided the first major leap forward. Heusler alloy crystals has opened the field of polarised neutron scattering³, which allows separation of nuclear and magnetic scattering, and a direct determination of the symmetry of magnetic excitations, the penalty however is a large intensity reduction.

The use of vertically and horizontally focusing monochromators and analysers allows significant increases in intensity at the expense of Q resolution^{4,5}. At a selection of discrete wavelength or wavelength bands higher order spurious scattering processes can be largely eliminated through the use of filters such as polycrystalline Be, BeO or poor mosaic pyrolytic graphite^{6,7}. The lack of tuneable filters does however constrain

the usable neutron energies, which may dictate an unfavourable intensity-resolution optimisation

The neutron spin echo method proposed by Mezei⁸ has been developed into a miniaturised version by Zeyen⁹ using optimally designed field coils. This design can be implemented on triple axis spectrometers yielding an improvement in relative energy resolution of three orders of magnitude.

Large sample tables and a steady progress in the range of sample environments available for neutron experiments is another significant factor for the success of the triple axis spectrometer.

The advances in computing have yielded instruments that are both more flexible and easier to use, i.e. it is possible to control both the instrument with focusing devices plus the sample environment and finally display the results including a first simple on-line display and analysis of the data.

The effect of monochromators, collimators and neutron optical elements on the resolution of the spectrometer and hence the expected intensity and peak shape is central to both the use and design of modern triple axis spectrometers. The first approaches were very useful for the understanding of kinematical focusing¹⁰ and for a detailed peak-shape analysis¹¹ of a spectrometer without focusing elements. A more general description uses a matrix formalism, and treats the different optical elements of a spectrometer as a series of phase space transformations. The latter description can be studied in a paper by Popovici and Yelon¹² and the references therein. Software enabling the use of these methods on-line during the experiment is available on most instrument computers.

Several unsuccessful attempts to bring the triple axis spectrometer beyond point by point inspection has been made by Brockhouse¹³, Dolling^{14,15} and Kjems¹⁶. There are several different reasons for the lack of success for these instruments. They were too complicated to operate, they were either too constrained in their settings due to bulky shielding around the different analyser systems or had too high a background because of a very open geometry. The improvement beyond point by point inspection is only practically useful if it allows several points covering a few resolution widths to be recorded at the same time, i.e. to measure a complete or a large part of a standard scan with only one setting of the spectrometer. The RITA instrument¹⁷, which is being implemented at Risø now, is an attempt to exploit the throughput of an area detector together with optimised beam optics to increase the efficiency of a crystal monochromator-analyser spectrometer. This instrument is based on the lessons from the previous attempts. It is re-designed all the way from the cold source and outwards, i.e. it is not just an add-on to an existing spectrometer, and furthermore it is believed that the actual hardware just is a start. Without the right software it will be used as a standard triple axis spectrometer (which is one limit of operation). The challenge is writing the software required for a simple user-friendly interface, which will be able to fully exploit the RITA capabilities. This will require efforts similar to the design efforts that has gone into the hardware.

The main emphasis in this paper has been on triple axis spectrometers at a continuous source, but some of the ideas described may also be relevant for an indirect geometry inelastic scattering instrument similar to PRISMA¹⁸, which might be implemented at a spallation source.

This paper was presented at an IAEA consultants meeting 16-19 March 1996 at Bhabha Atomic Research Centre, Bombay, India on the *Trends and Techniques in Neutron Beam Research for Medium and Low Flux Research Reactors*. It is therefore

not intended to be complete, but references have whenever possible been selected to complement each other and cover different important aspects of triple axis spectrometer design. The remaining part of the paper will be devoted to short discussions of the different components necessary for a triple axis set-up, with useful references for further reading.

Designing triple axis spectrometers

In most instances the task of designing a new spectrometer is severely constrained by the beam port, the space allocated to the spectrometer and the budget, i.e. the technical solutions chosen will be the result of a complicated set of compromises. For triple axis spectrometers especially it is important to bear in mind that ultimately it is the signal to noise ratio which determines whether an experiment is doable or not. i.e. even though shielding and shielding considerations are much less appealing to the designer, it is extremely important not to neglect this. This will in the future become even more important. For the most effective use of neutrons, the detector system will have to be rather open (area detectors) and the use of collimators should be avoided if an open geometry with clever optics can provide the required resolution with higher intensity in a different way.

Flexibility and modularity

A triple axis spectrometer is not an instrument that once build will stay in that same form forever. It will develop as new problems needs to be examined, new ancillary equipment, better optical elements or improved control software becomes available. The spectrometer components, control system and the system for visualisation and analysis of data should all be modular. With a flexible modular spectrometer design, improved performance can often been obtained at relatively low cost in term of components or equipment. The most essential ingredient is commitment, human resources and talents.

Cold, thermal and hot sources

The most useful moderators for triple axis spectrometers are cold and thermal sources. In heavy water moderated reactors the thermal source can either be a small container with D₂O placed as close to the core as possible in a beam tube passing tangential to the core, or direct view of the D₂O moderator. In H₂O cooled and moderated reactors a D₂O tank or a Beryllium reflector around the core is the ideal position for the sources. The temperature of the moderator in research reactors is normally around 320 - 350 K, and the corresponding spectrum will approximately follow a Maxwell-Boltzmann (MB) distribution with this characteristic temperature. (See fig. 1). A compilation of different cold source designs can be found in the proceedings from an *International Workshop on Cold Neutron Sources* held at Los Alamos, USA in 1990¹⁹. Three different designs of cold sources all operating at 20 - 35 K have demonstrated the best characteristics: boiling D₂, boiling H₂ or supercritical H₂. If the cold source has not been designed into the system from the start, the choice of system is often dictated by geometrical constraints in the reactor or the beam tube. Deuterium has a lower scattering cross section and lower absorption than hydrogen. i.e. a

deuterium source is generally larger (5 - 25 litres) and can be used with a re-entrant hole, in which the beam tube ends. The beam thus only sees the centre of the source and the corresponding spectrum is close to a true MB distribution (see fig. 1). The supercritical hydrogen system is a single phase system (operating at 15 bar), and its main advantage is the freedom to arrange the feed lines from the cryo-cooler to the source which can be required for horizontal installation in a small beam-tube. In the hydrogen sources (from 1 to a few litres of hydrogen) a larger proportion of the scattered neutrons escapes from the outer layers of the source without being fully thermalised, i.e. the distribution is MB with a tail towards thermal neutrons. Solid D₂O ice or methane cold sources should be avoided. From an intuitive licensing point of view these sources might sound more interesting, but in reality the hydrogen sources are better, safer and more reliable.

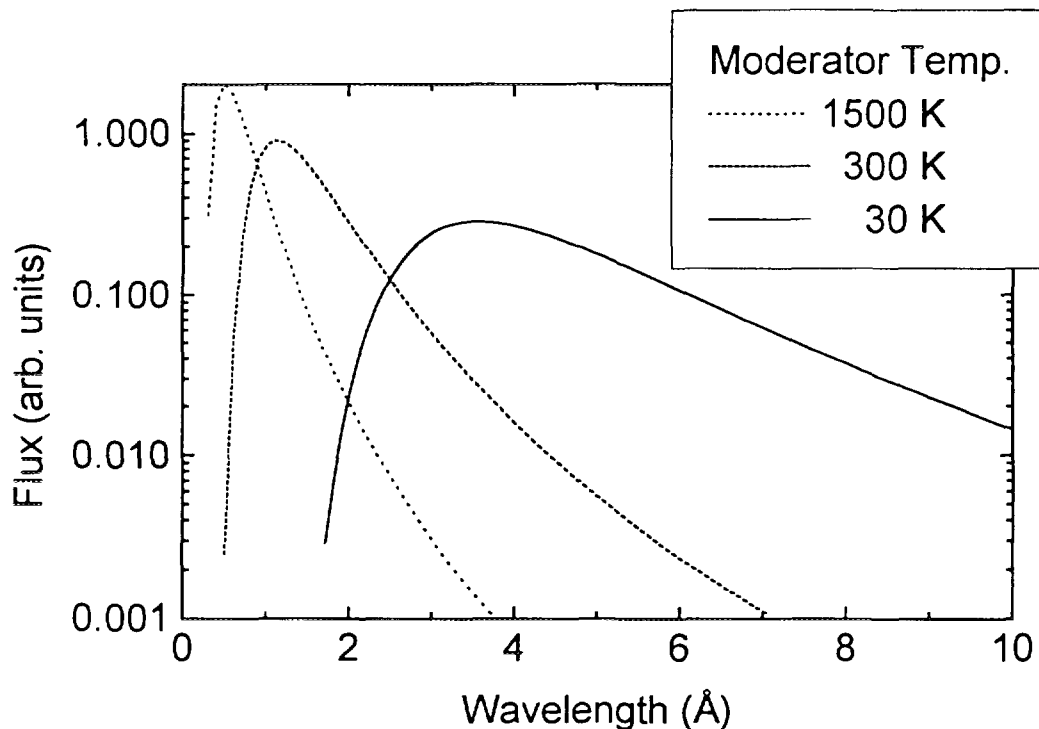


Fig 1. Maxwell-Boltzmann distributions functions for temperatures corresponding to the operating temperatures of cold, thermal and hot moderators.

A hot source is basically just a piece of graphite, which is heated to 900 - 1200 K by γ radiation from the core of the reactor. The use of crystal spectrometers for hot neutrons is however non-trivial. Hot neutrons are very penetrating and it is often difficult to make sufficiently effective shielding. The results are furthermore hampered by a multitude of possible spurious peaks. If not carefully shielded the installation of a hot source in an existing reactor could jeopardise the background of neighbouring instruments. It is my personal opinion that high energy inelastic scattering should be performed at pulsed sources. Hot to epithermal neutrons constitutes by virtue of the functioning of a spallation source a large proportion of the energy spectrum (high intensity), spurious effects are avoided by means of the time structure, and the source

is effectively switched off when the scattered neutrons are being detected (low background).

From the reactor to the monochromator - cleaning the beam

One of the most effective means to reduce the background on the spectrometer is to stop unwanted radiation as close to the source as possible. Fast neutron contamination can be strongly reduced by single crystal filters just after the source. The most commonly used such filters are sapphire, bismuth, quartz, silicon, beryllium or graphite. In figure 2 the neutron transmission of 2 different 10 cm single crystal sapphire filters attenuating fast neutrons is shown^{20,21}. For very good quality crystals the fast neutron contribution can be reduced by more than a factor of ten with a transmission of the wanted neutrons of the order of 80% or more.

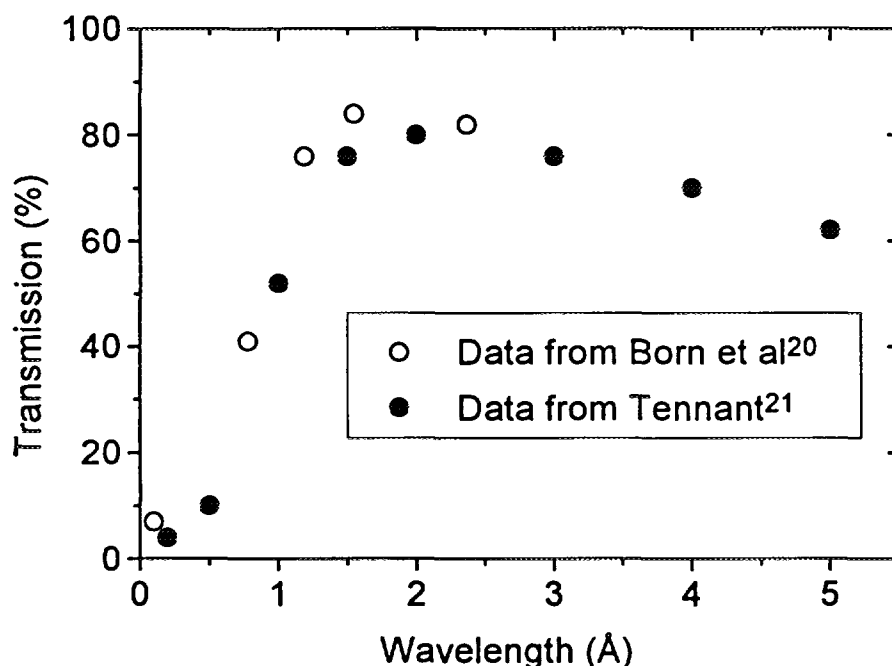


Fig. 2. Neutron transmission of 10 cm thick sapphire filters at room temperature.^{20,21}

Sapphire crystal filters have proven to be the best, but also most expensive filter for cold and thermal spectrometers^{20,21}. For cold neutrons a coarse low cost mechanical velocity selector filter can be used^{22,14} as a combined higher order filter and band-pass filter for the suppression of background from unwanted neutrons around the monochromator, Such a filter is tuneable, allows a large divergence to pass ($1^\circ - 2^\circ$) with a transmission in excess of 80% and a transmission of higher order neutrons of the order of 10^{-4} .

With a supermirror channel in the outer parts of the beam channel from the monochromator, a larger divergence can be transmitted and the background reduced because the window for the beam can be reduced in dimensions. A combination of these methods have reduced the fast neutron content on the monochromator position on RITA at Risø by a factor of 4 and increased the cold to thermal neutron flux by a factor between 2 and 3.

Supermirrors

Supermirrors are periodic layered structures, which has an effective critical angle m times larger than standard Ni. The enhancement is due to Bragg reflection from a multilayer structure. The reflectivity is in excess of 99% up to the critical angle for Ni ($Q_c \approx 0.02 \text{ \AA}^{-1}$ or $\theta_c \approx 6^\circ/\text{\AA}$). The reflectivity curve for a $m=4$ supermirror produced by Peter Böni at PSI²³ is shown in fig. 3. Supermirrors with a large number of bilayers are excellent for short guides with only one to a few reflections. For long guides a reflectivity in excess of 99% is required and so far only Ni coating or supermirror with small m has been used.

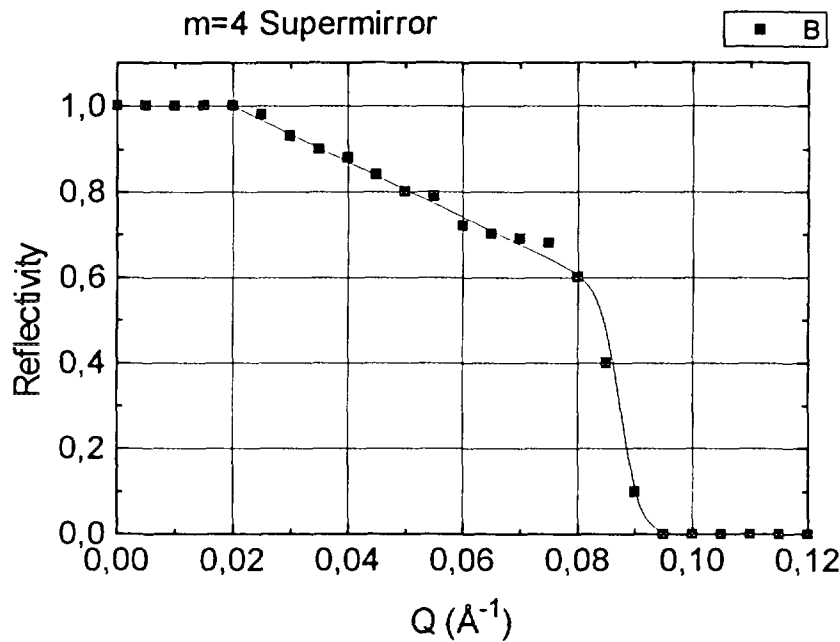


Fig. 3 Measured reflectivity of a $m=4$ supermirror guide prepared at the Paul Scherrer Institute²³. The line is a guide to the eye.

For cold neutrons tapered supermirror beam-channels or even better supermirror beam-channels which approximates to a parabolic shape can be use for real space focusing. Magnetised supermirrors can also be used as excellent beam polarisers.

Shielding materials

A compact design is often a wish for intensity reasons, but is in many cases a must, because of limited space available for the spectrometer. In this case it is especially important to use Monte Carlo code to simulate the actual radiation emerging through the beam tube from the reactor and the radiation scattered in the monochromator and its surroundings. Using this approach the optimum composition can be calculated for 1) the beam stop, 2) material which can be in the direction of the scattered beam from the monochromator and 3) more general purpose shielding material used in the monochromator drum. With the conditions relevant to the spectrometers at Risø, the optimal composition for the general purpose material²⁴ could be composed of a lead, boron and hydrogen mixture with a density of 4.6 g/cm^3 , 1 atom % of natural boron

and as much H as possible. We have produced this new composite material by extruding 12 mm balls consisting of approximately 50% Pb pellets and 50% polyethylene, and casting these balls in a mixture of H₂BO₃ and polyester. The composite material is substantially better than the old heavy concrete solution. The other materials in the monochromator drum has been selected in a similar way.

Monochromator/analyser crystals

The performance of a triple axis spectrometer depends crucially on the properties of the monochromator and analyser crystals. The reflected wavelength is determined by Bragg diffraction i.e.

$$\lambda = 2d \sin(\theta)$$

where d is the interplanar distance and θ is the Bragg angle. The wavelength bandwidth selected by perfect crystals are too narrow for most practical applications, unless they are used in open geometry's and elastically bent i.e. used as a focusing monochromator²⁵. The intensity can be increased substantially by selecting a bandwidth whose contribution to the overall resolution of the spectrometer is matched to the corresponding angular divergence to the beam.

The selected band-width can be tailored by introducing defects in the crystals:

$$\frac{\Delta\lambda}{\lambda} = \cot(\theta)\Delta\theta + \frac{\Delta d}{d}$$

where $\Delta\theta$ and Δd represent uncertainties in the orientation of the lattice planes (mosaic crystals) and the lattice spacing (gradient crystals) respectively. For a thorough review of the status of monochromator materials see the articles by Magerl²⁶, Götz²⁷ and the *Proceedings of the Workshop on Focusing Bragg Optics*⁵.

For resolutions in the meV range mosaic crystals are generally used. Beam divergences of the order of 0.5°, are matched to a mosaic width of the same value and results in a wavelength resolution of the order of 1%. The peak reflectivity for a perfect mosaic crystal is given by²⁷

$$R_{id} = \sqrt{\frac{4 \cdot \ln(2)}{\pi}} \frac{|F|^2 \lambda^3 n^2}{\sin(2\theta)\sin(\theta)} \frac{t}{\eta}$$

n is the number density, F the structure factor, t the sample thickness and η the mosaic width. Secondary extinction leads to saturation effects, and the actual reflectivity is given as:

$$R = \frac{R_{id}}{1 + R_{id}}$$

For wavelength above approximately 1.5 Å the best material is HOPG highly oriented pyrolytic graphite. The mosaic width is normally in the range 0.5 to 1 degree. Below 1.5 Å several candidates are used, plastically deformed Cu are produced rather standard for instance at the ILL. The main draw-back with Cu is the activation in a neutron beam, which makes Cu difficult to handle after irradiation. Be is another good candidate, but the technique to get good mosaic crystals is still not fully developed. Composite Ge monochromators²⁸ are developing rapidly at present and will in many cases replace Cu (Ge will not be activated in the beam). The important parameters for monochromator materials are: a large number density and coherent scattering length, a high Debye temperature and low absorption and incoherent cross section plus last but not least technical solutions to produce large crystals with a homogenous mosaic distribution.

In the table below a list of useful parameters for typical monochromator materials are given:

Table 1 List of properties for selected monochromator materials, a, c are lattice parameters, n the number density, θ_D the Debye temperature, σ_c and σ_i are the coherent and incoherent scattering cross-sections and μ_{abs} the linear absorption length. F is the structure factor²⁷.

Material	lattice	a c [Å]	n [Å ⁻³]	θ_D [K]	σ_c [b]	σ_i [b]	μ_{abs} [cm ⁻¹]	F ² [b]
PG (002)	hexagonal layered	2.46 6.71	0.057	420	5.50	0.01	0.0005	0.44
Ge (hkl) all odd all even	Diamond	5.66	0.044	366	8.80	0.20	0.058	0.35 0.70
Si (hkl) all odd all even	Diamond	5.43	0.050	658	2.16	0.04	0.04	0.09 0.17
Be	hcp	2.29 3.58	0.12	1160	7.53	0.06	0.0005	0.60
Cu	fcc	3.61	0.085	339	7.8	0.7	0.19	0.62

Gradient crystals are used for very good energy resolution (μeV), where the set-up is almost in a backscattering configuration.

The most commonly used **polarising monochromator** is the Heusler-alloy, which is quite difficult to make and have relatively small reflectivities. A very promising new development is the ³He filter polarisers²⁹. It is a cell with polarised ³He which only absorbs one spin state. This type of polariser is expected to be available within the next few years, and has the advantage that monochromatisation and polarisation are decoupled, i.e. we can use the best possible monochromator and focusing system in front of the filter. For long wavelength neutrons, magnetised supermirrors can be used to polarise the beam.

Focusing monochromator and analyser systems

The first focusing systems to be used were vertically focusing monochromators^{30,5}. They allow the use of smaller samples by increasing the flux on the sample by a factor of two to five at the cost of a degraded resolution out of the scattering plane. In most cases this has no adverse effects on the interpretation of the results. A vertically focusing analyser reduces the background by focusing the scattered beam onto a smaller detector.

The merits of horizontal focusing systems are similar - smaller samples, reduced background. In the horizontal plane we normally want better resolution. In many cases this can still be obtained using focusing as a tool to shape the resolution function. One method is to make monochromatic focusing, which maintains good energy resolution and a reduction in background by allowing a narrow diaphragm at the focal point in the incident beam.

A doubly focusing monochromator or analyser is a complicated mechanical set-up³¹, which combines the virtues of both horizontal and vertical focusing. A very powerful triple axis spectrometer using a doubly focusing monochromator and analyser and monochromatic focusing is installed at the ORPHEE reactor in Saclay and described in detail by Pintschovius⁴.

Spin Echo type triple axis spectrometers

Neutron spin-echo spectrometers were until recently huge instruments, but the development of new coil systems by Zeyen³², has miniaturised the set-up (small diameter coils), simplified the operation (the resolution is well behaved up to the maximum Fourier time), reduced the cost to about 10% of a complete triple axis spectrometer and allowed the use of large beam divergences (intensity gain). With this type of set-up a relative energy resolution of 10^{-5} has been obtained at the ISSP thermal triple axis spectrometer in Japan³³, i.e. a gain of three orders of magnitude over standard triple axis spectrometers. On the proposed superconducting version at the ILL a relative energy resolution of 10^{-6} is expected⁹. The only intensity penalty stems from the fact that polarised neutrons are used. At the ILL a new spectrometer TASSE (Triple Axis Spectrometer with Spin Echo) is being developed. With this instrument complete phonon focusing (matching both slope and curvature) should be possible for the study of excitation lifetimes⁹. Ultra-high resolution measurements using a spin-echo add on to a triple axis spectrometer is however best suited at a high flux reactor.

TAS with Elasticity bent perfect monochromator and analyser

Kulda³⁴ at the ILL has demonstrated that a triple axis spectrometer with elastically bent perfect Si (111) monochromator and analyser crystals can be a cheap alternative to and in some cases outperform a standard Soller collimated triple axis spectrometer with flat PG (002) monochromator and analyser crystals. With properly optimised vertical and horizontal focusing very efficient real space focusing can be obtained, and the Soller collimators necessary for a similar resolution on the PG (002) system can be omitted. The Silicon set-up has furthermore the advantage that second order contamination is eliminated. If larger samples are available, then a system with a mosaic monochromator and analyser are in general more flexible.

Multi-element analyser system

An attempt to get beyond point by point inspection is realised in the analyser set-up for RITA¹⁷. This paragraph is an update on the description in the paper by Mason¹⁷. The single analyser-detector pair of a conventional triple axis is replaced by an array of seven independently orientable, flat vertical vanes of pyrolytic graphite, which scatter neutrons onto a microstrip area detector. By rotating each blade independently, as well as the entire array, it will be possible to choose different modes of operation. A flat analyser, together with Soller slit collimators and an electronically selected window in the centre of the area detector is the standard triple axis geometry - and is one limit of operation. Removing the collimators one can employ the standard horizontal focusing geometry onto the centre of the detector (shown schematically in fig. 5a). In this case each analyser blade is set for the same energy, all of them focus on the same point on the detector, and the analyser array is set at an angle ψ_A with respect to the scattered beam:

$$\tan(\psi_A) = \frac{1}{\left(\frac{AD}{SA \cdot \sin(2\theta_A)} + \cot(2\theta_A) \right)}$$

SA is the sample to analyser distance, AD is the analyser to detector distance, and θ_A is the analyser Bragg angle for the desired neutron wavelength. (see fig. 4a). Here the integrated intensity in the spot in the centre of the detector is an integral in \mathbf{Q} space at constant energy transfer, i.e. with individually adjustable vanes, monochromatic focusing can be obtained without having $AD = AS$. Tests of this analyser set-up - for both incoherent elastic scattering from vanadium and inelastic magnetic scattering - have shown a factor of five increase in intensity in point focusing mode when compared to a flat analyser. The vanadium energy width was slightly better than for the flat analyser.

The virtues of horizontally focusing analysers for measurements where \mathbf{Q} resolution can be sacrificed but good energy resolution is required have been known for many years. RITA, because of its area detector, can also operate in line focusing mode (shown in fig. 4b) where the analyser blades are dispersed across the face of the detector. In this case a constant energy scan perpendicular to the \mathbf{k}_f (\mathbf{k}_f is the \mathbf{k} vector of the outgoing beam) runs across the detector so that the gain in efficiency of horizontal point focusing is realised without the loss in \mathbf{Q} resolution (the scan is actually an arc and not a line, but this is not a significant effect given the finite resolution).

The resolution of each analyser is determined by its mosaic spread and the effective distance collimation (1 degree for a point sample at 60 cm with a 1.5 cm wide analyser at 74 degrees $2\theta_A$). Because the angular separation of the analysers is the same as the collimation, each point is correctly spaced with respect to the size of a resolution element. With seven vanes an area detector, 15 cm wide, will accommodate the beam. Of course this gain is only useful if the background does not increase too much. i.e. the front end of the instrument must be carefully designed.

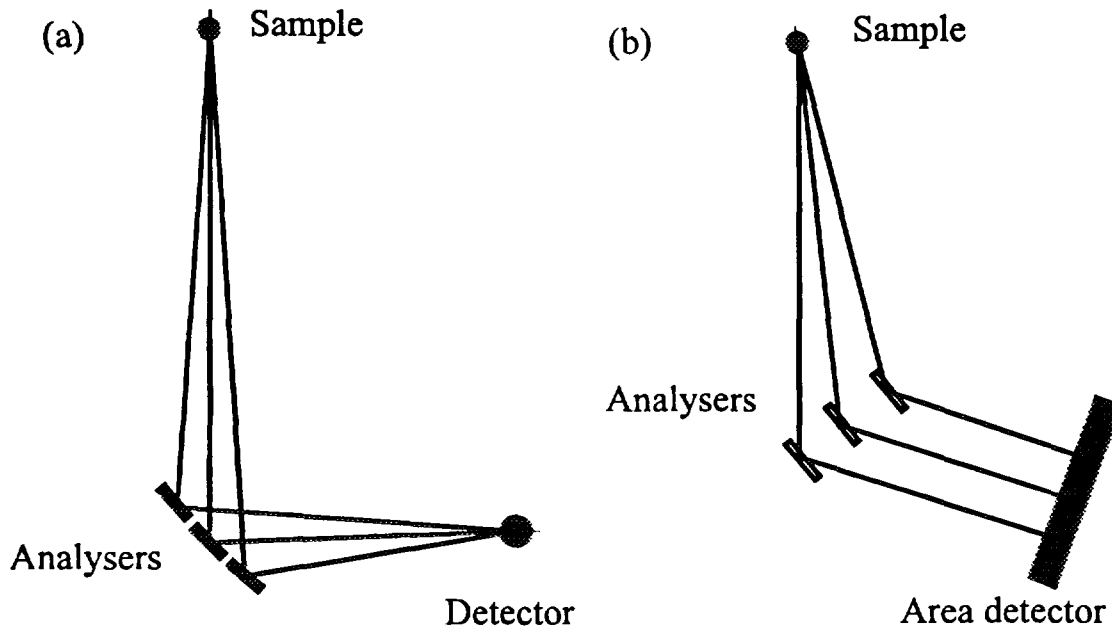


Fig. 4 Schematic illustration of a multi-element analyser operating in a) point focus and b) line focus mode. For clarity only three blades are shown.

In addition the analyser tank will be evacuated (with a sapphire window) to prevent neutrons from scattering off air and into the area detector which could otherwise be a problem when operating without Soller slit collimators (air scatters about 5 % per metre due to the incoherent cross section of nitrogen). Tests of the analyser tank have shown that the background per unit detector volume is lower than on the existing Risø triple axis machines which in part can be attributed to the lack of wedges in the design. Measuring at more than one Q and ω is only useful if it can be arranged so that the additional data is at interesting locations (this was part of the problem with the Chalk River multi-analyser system).

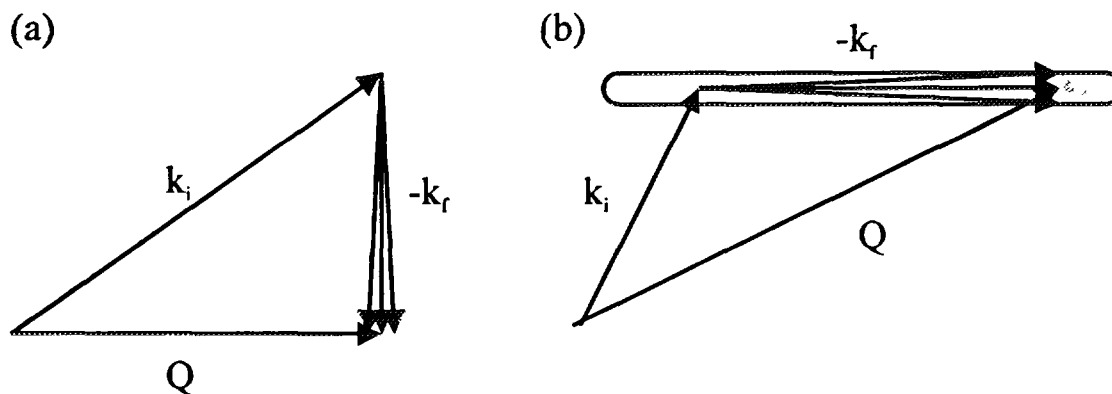


Fig. 5 Scattering diagrams in reciprocal space for a constant energy focusing analyser showing a) orientation to produce a constant E scan aligned to approximately coincide with a high symmetry direction and b) a scan across a two dimensional rod of scattering in a two dimensional material. The array could be operating in point focus mode in which case an integral over the Q 's shown would be measured or in line mode in which case the scan would be resolved across the detector face.

In most condensed matter systems the scattering of interest is located in a small region of the four dimensional \mathbf{Q}, ω space, the single resolution element spacing of the RITA analyser makes it ideally suited to a wide range of problems. By setting \mathbf{k}_f perpendicular to a high symmetry direction in the crystal (as shown in fig. 5a) it is possible to perform a constant E scan in that direction.

The wavevector of the centre of the scan determines which \mathbf{k}_f satisfies this condition, i.e. a tuneable velocity selector higher order filter is needed in the incident beam. Figure 5b illustrates another situation, that of a two dimensional material where the scattering is independent of wavevector along a rod in reciprocal space. In this case the area detector scans at constant energy perpendicular to the rod and \mathbf{k}_f can be selected based on resolution considerations alone since the degree of freedom needed to satisfy the scan condition is the displacement along the rod. Of course one can construct many different geometries subject to kinematic constraints, i.e. in general both \mathbf{Q} and ω vary across the detector. A constant \mathbf{Q} scan is however not possible in a single setting.

It is thus possible to focus a dispersive mode over the entire detector. Provided the scan is dispersed uniformly across the detector the intensity can be binned to optimise for intensity (summing the detector) or resolution (retaining the same number of bins as there are analysers) after the experiment is finished. Between these limits there is the possibility for a continuous trade off between intensity and resolution. The vertical detector elements can be treated in the same way although in that case only the component of \mathbf{Q} perpendicular to the scattering plane is varying. As a cheap alternative the detector could be made from seven vertical ^3He tubes.

Control system and software

Today the cost of a control computer for a spectrometer is negligible compared to the cost of the rest of the system and advances in computer performance is so fast that the control computer should be a module in the system which can be easily changed, i.e. the hardware to control detectors, motors, ancillary equipment etc. should not be integrated as cards on the computer bus. A solution with a personal computer interfaced to the hardware by means of interfaces like VME, IEEE or RS232 is a flexible solution, which allows upgrades and replacements of the individual components without changing the whole system.

The more complex the system, the more essential will the software be. The experimentator should focus his attention on the features in \mathbf{Q}, ω space he wants to study, and which resolution he requires. The setting of the spectrometer which most efficiently provide the answer, should then be suggested by the control system, and during the actual data taking the results should be optionally visualised either directly as the observed counts on the detector or in the appropriate cut in \mathbf{Q}, ω space. The latter is a challenge and a task which is often underestimated, but which will be essential for the success of the investment.

Conclusion

The triple axis spectrometer is a versatile and powerful tool for probing the dynamics of single crystals. It has provided key information for our understanding of magnetism, superconductivity, phase-transitions, ion diffusion, lattice dynamics etc.

The excitations of crystals are in general either delta functions or narrow peaks centred around dispersion surfaces, i.e. information is concentrated in a limited fraction of \mathbf{Q}, ω

space. Selectively focusing on a series of single points in this four-dimensional space has proven to be an efficient method, because each point has a large information content. Measurements based on a series of point by point scans are furthermore simple to control and easy to analyse. Hence the large success of the triple axis spectrometer. Improvement beyond point by point inspection on triple axis spectrometers will only be practically useful, if it allows several points approximately a resolution width apart to be recorded at the same time, i.e. to measure a complete or a part of a standard scan with one setting of the spectrometer. A multi-filament analyser and an area-sensitive detector, or a row of 7 to 10 single detectors is a suggestion for such an improvement. The same set-up would also allow a more efficient mapping of more extended regions in Q , ω space from systems where the scattering function is a smoothly varying function of Q and ω , (e.g. powders, disordered systems, spin fluctuations in High temperature superconductors, broad quasielastic scattering etc.).

A triple axis spectrometer is also a versatile and flexible instrument which can be used in several different modes and for test of new instrumental concepts. In most small and medium flux reactors triple axis spectrometer are often also used as a diffractometer (for very weak scatterers where the background is critical), a diffuse scattering spectrometer (especially when fitted with an area detector), a reflectometer or to test reflectometer or SANS concepts. In general a triple axis spectrometer is also one of the best spectrometer types for training purposes.

A triple axis spectrometer should be build in a modular fashion, i.e. as a start a simple version could be build, and later the different axis, monochromator-analyser systems, guide optics or detector systems can be upgraded when improved components or funds are available. From the initial design it is however very important to carefully design the shielding for maximum efficiency, and choose an overall design, which is prepared for changes or upgrades.

The triple axis spectrometer is most powerful for cold and thermal neutrons. If a cold source is planned then hydrogen or deuterium moderated cold sources are to be preferred. Solid D_2O ice or methane should be avoided. From an intuitive licensing point of view the latter sources might sound more interesting, but in reality the hydrogen sources are safer, better and more reliable. A hot source for a crystal monochromator-analyser triple axis spectrometer at a low or medium flux reactor is less attractive.

On the triple axis spectrometer provisions should be made for the use of several methods for focusing optics. Monochromators focusing in the vertical plane is a minimum requirement. Provisions should be made for use of polarising filters i.e. magnetic materials should be avoided in and just around the beam channel. Ultra-high resolution measurements using a spin-echo add on to a triple axis spectrometer can not be recommended at a low or medium flux reactor. The possible flux will be to low to justify this extra investment.

Many new developments are pushing triple axis spectroscopy into new areas of parameter space and increased intensity and effectiveness is allowing smaller samples and weaker cross sections to be investigated. triple axis spectroscopy at steady state sources is an open an lively field where scientists with new ideas can make substantial

contributions, and triple axis spectrometers will continue to be the instrument of choice for many experiments, especially at good reliable reactors with cold sources

One of the big challenges in the future will be how triple axis like experiments can be performed on new powerful spallation sources, and how some of the lessons and methods learned during the development of modern steady state instrumentation's can be used either directly or indirectly by stimulating improvements in instrumentation at spallation neutron sources, and vice versa

Acknowledgements

During the whole RITA project I have had very frequent and long discussions with T E Mason, G Aeppli, D F McMorrow, J Søgård, B Lebeck and J K Kjems Their support, contributions and advice has been absolutely essential for the project and cannot be over estimated Stimulating discussions, advice and pre-prints from C Broholm, P Boni, G Eckold, B Hennion, J Kulda, A Schroder, U Steigenberger, F Tasset and C M E Zeyen are gratefully acknowledged

References

- ¹ B N Brockhouse, in *Inelastic Scattering of Neutrons in Solids and Liquids*, IAEA Vienna, (1961) 113
- ² T Riste and K Otnes, *Nucl Instr and Meth* 75 (1969) 197
- ³ R M Moon, T Riste and W C Koehler, *Phys Rev B* (1969), 920
- ⁴ L Pintschovius, *Nucl Instr & Meth* A338 (1994) 136
- ⁵ Proceedings of the Workshop on Focussing Bragg Optics Braunschweig, 1993, *Nucl Instr & Meth* A338 (1994)
- ⁶ B N Brockhouse, S Hautecler and H Stiller, *Proc Int Summer School Mol*, (1964) 580
- ⁷ J Bergsma and C van Dijk, *Nucl Instr and Meth* 51 (1967) 121
- ⁸ F Mezei (ed) *Neutron spin echo*, Lecture notes in Phys 128 (Springer, Berlin) 1980
- ⁹ C M E Zeyen and K Kakurai to be published in *Journal of Neutron Research*
- ¹⁰ H Bjerrum Møller and M Nielsen, in *Instrumentation for Neutron Inelastic Scattering Research*, IAEA Vienna, (1970) 49
- ¹¹ M J Cooper and R Nathans, *Acta Cryst* , 23, 357 (1967)
- ¹² M Popovici and W B Yelon, *Journal of Neutron Research* vol 3 no 1 (1995) 1
- ¹³ B N Brockhouse, G A DeWit, E D Hallman, and J M Rowe, in *Neutron Inelastic Scattering*, IAEA Vienna, (1968) 259
- ¹⁴ G Dolling, *Proc of the Enrico Fermi International School of Physics, Course LV*, Academic Press, New York, (1975) 176
- ¹⁵ G Dolling, in *Dynamical Properties of Solids*, Vol 1, Eds G K Horton and A A Maradudin, North Holland, Amsterdam, (1974) 566
- ¹⁶ J K Kjems and P A Reynolds, in *Proceedings of the 1972 IAEA Meeting on Inelastic Neutron Scattering*, IAEA-SM-155/F-4, IAEA Vienna, (1972) 733
- ¹⁷ T E Mason, K N Clausen, G Aeppli, D F McMorrow and J K Kjems *Can J Phys* 73 (1995) 697

- ¹⁸ U. Steigenberger, M. Hagen, R. Caciutto, C. Petrillo, F. Cilloco, and F. Sachetti, *J. Phys: Condens. Matt.* **53** (1991) 87
- ¹⁹ Proceedings from the International Workshop on Cold Neutron Sources, March 5-8, Los Alamos, New Mexico, USA. **LA-12146-C** 1990
- ²⁰ R. Born, D. Hohlwein, J. R. Schneider and K. Kakurai, *Nucl. Inst. and Methods* **A262** (1987) 359
- ²¹ D. C. Tennant *Rev. Sci. Inst.* **59 2** (1988) 380
- ²² W. Wagner, H. Friedrich and P. Wille, *Physica B* **213&214** (1995), 963
- ²³ P. Böni (Private communication)
- ²⁴ J. Søgård Internal Risø note
- ²⁵ J. Kulda, *Physica B* **213&214** (1995) 926
- ²⁶ A. Magerl, *Physica B* **213&214** (1995) 917
- ²⁷ G. Eckold (Private communication)
- ²⁸ J. Axe, S. Cheung, D. E. Cox, L. Passell, T. Vogt and S. Bar-Ziv. *Journal of Neutron Research* Vol. 2 Number 3 (1994) 85
- ²⁹ F. Tasset, *Physica B* **213&214** (1995) 935
- ³⁰ T. Riste, *Nuclear Instrum. Methods*, **86** (1970) 1
- ³¹ W. Bühner, *Nucl. Instr. & Meth.* **A338** (1994) 44
- ³² C. M. E Zeyen and P. C. Rem to appear in *Measurement Science and Technology*
- ³³ T. Takeda, S. Komura, H. Seto, M. Nagai, H. Kobayashi, E. Yokoi, T. Ibisawa, S. Tasaki, C. M. Zeyen, Y. Ito, S. Takahashi and H. Yoshizawa, *Physica B* **213&214** (1985) 863
- ³⁴ J. Kulda and J. Saroun, Submitted to *Nucl. Instr. & Meth. A*

NEXT PAGE(S)
left BLANK



M.T. REKVELDT

Interfacultair Reactor Instituut,
University of Technology Delft,
Delft, Netherlands**Abstract**

The neutron depolarisation technique is based on the change of polarisation of a polarised neutron beam in three dimensions after transmission through magnetic substances. This change yields the mean domain size, the mean square direction cosines of the domain magnetisations and the mean magnetisation. The method is complementary to other neutron scattering techniques with respect to the size of the inhomogeneities to be studied as well as the dynamic range accessible. The principles of the technique will be explained in some detail and demonstrated with a number of applications.

1. Introduction

The application of neutron depolarisation started already in 1941 by Halpern and Holstein [1] theoretically and Burgy et al in 1950 experimentally [2]. Contrary to neutron scattering and small angle neutron scattering (SANS) the method has never developed into a widespread application. At present, neutron depolarisation is exploited at a few places in the world. Without aiming to be all-embracing, I would like to mention the work by Drabkin, Okorokov et al [3,4] and the theoretical work by Maleyev, Toperverg et al. [5] in Leningrad and also by Rauch [6] and Badurek et al [7] in Vienna and all references therein. The range of sizes probed by neutron depolarisation is between 0.02 μm and macroscopic dimensions, i.e. complementary to and overlapping SANS. In the range above 0.1 μm the application of SANS fails by a lack of sufficient resolution. However, the application of the neutron depolarisation technique is confined to magnetic phenomena and enables one to determine magnetic inhomogeneities as domain size or correlation length of the local magnetisation, the mean square direction cosines of the domain magnetisation directions and the mean magnetisation vector [8] and their time dependence. Further it should be noted that in a ND experiment one single intensity measurement determines a correlation length while in a SANS experiment the whole momentum dependence is needed for this information.

In the next sections the neutron depolarization technique will be treated and an overview will be given about the applications, without aiming to be all embracing. A few applications in materials research will be discussed in more detail.

2. Interaction of neutron spin with magnetic induction

Because of the magnetic moment of the neutron the magnetic interaction of the neutron spin with a magnetic field is described by the Hamiltonian $\hat{H} = -\hat{\mu} \cdot \mathbf{B}$ where $\hat{\mu} = \gamma \mu_N \hat{s}$ and $\hat{s} = \frac{1}{2} \hat{\sigma}$. Using basic quantum mechanics the time derivative of the moment operator can be described by,

$$\frac{d\hat{\mu}}{dt} = -\frac{i}{\hbar} [\hat{\mu}, \hat{H}] \quad (1)$$

The square brackets indicate the commutator of the two included operators. Working out this equation leads exactly to the classical Larmor equation of precession of the spin operator around the magnetic induction \mathbf{B} . The average of this operator can be defined as the classical polarisation vector $\mathbf{P} = \langle \hat{\sigma} \rangle$ and is described by,

$$\frac{d\mathbf{P}}{dt} = \gamma(\mathbf{P} \times \mathbf{B}) \quad (2)$$

The solution of this equation is the Larmor precession of the polarisation vector around the field \mathbf{B} . Although according to quantum mechanics only one spin component can be measured at a certain time, all three components can be determined successively without any problem. The Larmor precession frequency is given by $\omega = \gamma |\mathbf{B}|$. Except for the construction of polarisation rotators this precession is the basic principle of the neutron depolarisation technique and also of the neutron spin echo technique. Both techniques make use of the proportionality of the interaction time t of the neutron with any field and the product of interaction length l and neutron wavelength λ ($t = l/v \equiv ml\lambda/h$). With the interaction time also the Larmor precession angle $\phi = \omega t$ is determined. Another essential feature of these techniques is the use of neutron polarizers for polarisation and analysis of the polarisation.

In case of a interaction with a time dependent field the solution of equation (3) can be approximated by successive iteration. In formula,

$$\mathbf{P}(t) = \mathbf{P}(0) + \gamma \int dt [\mathbf{P}(0) \times \mathbf{B}(t)] + \gamma^2 \iint dt dt' [[\mathbf{P}(0) \times \mathbf{B}(t)] \times \mathbf{B}(t')] + \dots \quad (3)$$

where the third term on the right hand side is assumed to be much smaller than the first two terms. The first two terms describe the normal Larmor precession around the average magnetic induction while the third represents the deviations from the average precession, which however is still not depolarisation. After averaging this term over the beam cross-section with different $\mathbf{B}(t)$ paths this leads to depolarisation of the beam.

In the above treatment only magnetic interaction is assumed. In case of interference of nuclear and magnetic interaction and correlations between the nuclear and magnetic inhomogeneities, new more complicated depolarisation effects can be expected which will not be treated here.

3. Neutron depolarisation

Measuring Method

In this technique use is made of a polariser P and an analyser A in combination with two polarisation rotators R_1 and R_2 (see schematic view in fig.1). Each rotator consists of two mutually perpendicular coils in which a magnetic field can be generated of any required size and direction in a plane perpendicular to the neutron beam. In this way the precession of the polarisation vector can be chosen in such a way that any required orientation of the polarisation can be obtained [8].

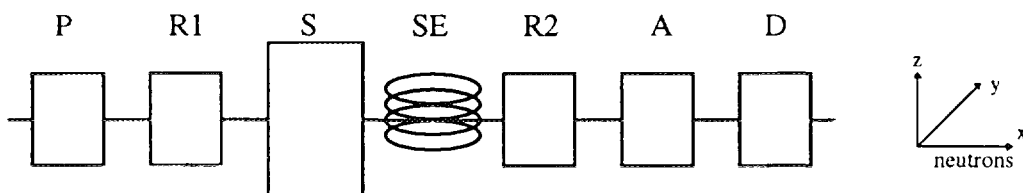


Fig.1 Schematic view of the depolarisation set-up. Here P and A are the polariser and analyser respectively, R_1 and R_2 polarisation rotators, S the sample holder, SE a spin echo coil to compensate for large rotation angles in the sample holder and D is the neutron detector.

In the same way any desired component of the polarisation at the sample position can be rotated to the analysing direction determined by the analyser magnetisation direction. In this way a (3×3) depolarisation matrix can be measured successively that describes the 3-dimensional change of the polarisation vector. To avoid depolarisation by the wavelength spread in the beam, just behind the sample in the sampleholder a spin-echo compensation coil (SE) can be applied to compensate for large rotation angles in the sample, e.g. by strong magnetised samples [9]. The current applied in the SE coil is adjusted to obtain optimal polarisation and doing so the current is a direct measure for the mean magnetisation of the sample. The use of the SE coil creates also the possibility to carry out 3 dim analysis on magnetised media while using a white neutron beam, with the advantage of measuring with very high neutron intensities. All effects together can be described by the formula,

$$\mathbf{P}(t) = \mathbf{D} \mathbf{P}(0) \quad (4)$$

The matrix \mathbf{D} contains now the depolarisation of the sample and the rotation by the magnetisation and spin-echo coil. The matrix is determined from the measured intensities by,

$$D_{ij} = (I_s - I_{ij}) / (I_s - I_m) \quad (5)$$

with I_s and I_m the intensities of the fully depolarised and polarised beam respectively and I_{ij} the intensity of the beam with $j, i = x, y$ or z . referring to the direction of polarisation and analysis respectively. The detected neutron pulses are eventually stored in a multichannel in order to measure the time dependence of the depolarisation matrix. The start signal of the latter can be synchronised with a periodic magnetic field or other periodic parameter of the sample. The optimal real time resolution amounts $\sim 5\mu\text{s}$.

Neutron Depolarisation in systems with known average domain structure.

In the study of inhomogeneous magnetic media the measured depolarisation matrix \mathbf{D} can theoretically be described as the solution of the Larmor equation as described in equation (3), but sometimes the knowledge of the system in study allows one to describe the theoretical depolarisation matrix as a product row of matrices as given in equation (6),

$$\mathbf{P}(t) = \prod_{i=1}^N \mathbf{D}_i \mathbf{P}(0) \quad (6)$$

where some preknowledge of the system can be used to describe the product row of matrices in a number of parameters which can be determined by fitting the measured matrix with the theoretical expression of equation (6). A maximum of 9 parameters can be measured in this way. This approach has been used in the analysis of depolarisation in an amorphous ribbon $\text{Fe}_{40}\text{Ni}_{40}\text{B}_{20}$ which consists of three magnetic layers, two surface layers with local magnetic anisotropy perpendicular to the layer and a central layer with easy axis in the plane of the layer [10]. The effect of each of them on the polarisation vector can be described by a simple modified rotation matrix.

Neutron Depolarisation in systems with random magnetic correlations.

More generally the theoretical depolarisation matrix is found by solving eq.(3) for the case of zero net magnetisation in the small angle approximation which is here equivalent with the Born approximation in scattering theory. This leads to [11],

$$\mathbf{P}' = \mathbf{P} - \frac{cL}{W} \iiint_W d^3\mathbf{r} \int_{z_0}^z dx' [(\mathbf{B}(\mathbf{x}) \cdot \mathbf{B}(\mathbf{x}')) \mathbf{P} - (\mathbf{P} \cdot \mathbf{B}(\mathbf{x}')) \mathbf{B}(\mathbf{x})] + \dots \quad (7)$$

In this expression the integrals over t and t' have been replaced by the integrals over the position coordinate x and x' . The terms $\mathbf{B}(x)$ and $\mathbf{B}(x')$ are short hand notation of $\mathbf{B}(x,y,z)$ and $\mathbf{B}(x',y,z)$. Moreover the averaging over the cross-section of the beam and one integral over x have been combined in the integral over a small part L_w of the sample volume W . From this expression the elements of the depolarisation matrix D_i can be found,

$$D_{ij} = \delta_{ij} \left(1 - cL_w \xi^0\right) + cL_w \alpha_{ij}^0 \quad (8a)$$

with

$$\alpha_{ij}^0 = \frac{1}{W} \int_W d^3\mathbf{r} \int_{z_0}^z dx' B_i(x) B_j(x') \quad (8b)$$

$$\xi^0 = \sum_i \alpha_{ii}^0$$

More generally in a sample magnetised in the y -direction, the depolarisation matrix under certain conditions is given by the matrix elements,

$$\begin{aligned} D_{xx} &= D_{zz} = \cos \varphi \exp\left[-cL_s(\xi^0 - \alpha_{xx}^0)\right] \\ D_{xz} &= -D_{zx} = \sin \varphi \exp\left[-cL_s(\xi^0 - \alpha_{xx}^0)\right] \\ D_{yy} &= \exp\left[-cL_s(\xi^0 - \alpha_{yy}^0)\right] \end{aligned} \quad (9)$$

with L_s the total sample thickness in the neutron direction and

$$\begin{aligned} \alpha_{ii}^0 &= \frac{8\pi^4}{W} \int_Q \Delta B_i(\mathbf{q}) \Delta B_j(-\mathbf{q}) d^2\mathbf{q} \\ \xi^0 &= \frac{8\pi^4}{W} \int_Q \Delta B(\mathbf{q}) \Delta B(-\mathbf{q}) d^2\mathbf{q} \\ \Delta B(\mathbf{q}) &= \frac{\mu_0}{(2\pi)^3} \int_W \Delta B(\mathbf{r}) e^{i\mathbf{q}\cdot\mathbf{r}} d^3\mathbf{r} \\ \Delta B(\mathbf{r}) &= [\mathbf{q}' \times [\Delta \mathbf{M}(\mathbf{r}) \times \mathbf{q}']] \end{aligned} \quad (10)$$

and $\varphi = \langle B \rangle L_s c_1$

with $c_1 = 4.7 \cdot 10^{14} \lambda \text{ m}^{-2} \text{ T}^{-1}$ and $c = c_1^2 / 2$

Expressions (9) have been derived in the Larmor approach assuming isotropic depolarisation in the xz -plane. In the scattering approach it is not possible to derive these expressions for a magnetised sample because the Born approximation is not valid in the case of large continuous phase rotation in passing the sample. Using the Eikonal approach [12,13,14] it appears possible to derive the depolarisation formulae also in the magnetised case, from which the intuitive Larmor approach for this case can be verified.

In expressions (10) \mathbf{q} is a vector in the 2 dimensional reciprocal space Q perpendicular to the beam direction and \mathbf{q}' its unit vector. The expressions (10) can be found from

equations (8) by using the Fourier representation of the magnetic induction fluctuation. This representation has the advantage that stray fields from a certain magnetisation distribution are included already in the expressions by means of the vector expression of $\Delta\mathbf{B}(\mathbf{r})$ in eq.(10) which contains no field contribution any more. The latter is the result of applying Maxwell's equations on $\mathbf{B}(\mathbf{r})$. A more rigorous treatment of the depolarisation in terms of neutron scattering theory shows that the reciprocal vector \mathbf{q} can directly be identified with the elastic neutron momentum transfer vector. The correlation length ξ^0 of eq.(10) is in scattering terms nothing else than the total magnetically scattered intensity into the detector. The acceptance angle of the analyser-detector system expressed in \mathbf{q}_{\max} in the integral boundaries of ξ^0 of eq.(10) determines in this way the smallest correlation length which can be determined with this method. From equation (10) it appears that ND can be compared directly with SANS results. The correlation parameter ξ^0 can be identified with the fluctuations of $\mathbf{B}(t)$ around the average $\langle\mathbf{B}\rangle = m\mathbf{B}$. These fluctuations can be approached by $\xi^0 = B_s^2(1-m^2)\delta$, where δ is a correlation length over which the magnetic fluctuations are more or the less homogeneous. In ferromagnetic domain structures δ can be identified with the mean domain size. The ratio $\gamma_i = \alpha_i^0 / \xi^0$ gives the mean square direction cosines of the fluctuations along $i = x, y$ and z axis. A trivial correlation in the magnetic sample imposed by the Maxwell laws $\text{div } \mathbf{B} = 0$ and $\text{rot } \mathbf{H} = 0$ and translated in Fourier space by $\mathbf{B}(\mathbf{r}) = [\mathbf{q}' \times [\mathbf{M}(\mathbf{r}) \times \mathbf{q}']]$ in equation (11), causes that also in further isotropic systems not $\gamma_x = \gamma_y = \gamma_z = 1/3$ is measured but $\gamma_x = 1/2$ and $\gamma_y = \gamma_z = 1/4$ if x is the transmission direction of the neutron beam.

Polarisation rotation in magnetised media.

From equation (10) the precession angle ϕ is proportional to the $\langle\mathbf{B}\rangle d$ where $\langle\mathbf{B}\rangle$ is spatially defined within the margins of the sample thickness d . What is the situation in case $\langle\mathbf{B}\rangle$ is directed parallel to the neutron beam? In this case also precession occurs in the demagnetisation fields of the sample and one may wonder what is actually measured in the Larmor precession. For this purpose one may consider the line integral $\int B_x dx$ along a neutron path. Neglecting the contributions in infinity one can easily derive,

$$\int_{-\infty}^{\infty} B_x dx = \oint_S \text{rot} \mathbf{B} \cdot d\mathbf{S} = \mu_0 \oint_S \text{rot} \mathbf{M} \cdot d\mathbf{S} = \mu_0 \int M_x dx = \mu_0 M d \quad (11)$$

which means that also in this case without currents ($H=0$) the measured rotation angle corresponds to the magnetisation in product with the thickness of the sample and the effects of the demagnetisation fields cancel.

4. Application of ND in magnetic materials

The ND has been applied in numerous subjects in the course of the years. Some of them are listed below. As an example the application in HTS YBACU will be discussed in more detail.

Thin Films

In thin magnetic films neutron depolarisation can be applied in studying the domain structure perpendicular as well as parallel to the film [15]. In this respect neutron depolarisation is also complementary to neutron reflectometry which studies the atomic and magnetic structure of the film perpendicular to the surface [16]. The application range of the reflection technique is typically from atomic dimensions up to 0.1 μm perpendicular to the film, while the range of the neutron depolarization starts above 0.01 μm , however in all directions.

Amorphous ribbons under stress

Amorphous ribbons appear to be consist of a layered domain structure, caused by a stress transition from compressive to tensile stress going from the surface to the

centre of the ribbon. with 3 dim. ND it appears possible to analyse this domain structure in detail and by doing this as a function of applied stress on the ribbon, it appears possible to scan the stress distribution in the ribbon [10]. Also from the wave length dependence of 1 dim. ND with the polarisation making an angle with the average magnetisation of the ribbon, similar although less informative results can be obtained [17].

Small Particle Systems, [11]

In these systems the magnetic correlation between particles in remanent state and field dependent can be determined, together with the mean direction cosines of the local particle magnetisation directions and the average magnetisation [18]. Also the field history and effect of particle shapes appear important on the correlations [11]. The measured parameters are important for characterisation of the microstructure in magnetic recording materials and ferrofluids.

Time dependent ND

Also in the dynamics of materials, neutron depolarization is complimentary with inelastic neutron scattering. However, the dynamics studied with neutron depolarization are measured in real time in contrast with the scattering techniques. Dynamic experiments are carried out by applying a periodic action to the sample such as a magnetic field or a tension and studying the response of the domain structure on this action by measuring the neutron intensity in periodically triggered time channels [19]. With this technique a time resolution of about 5 μ s can be obtained. Because of the limitation in time scale at short times time dependent neutron depolarization has up to now only been applied successfully to eddy current limited domain wall movements and to time dependent rotation of induction in high T superconductors and flux creep [20].

The eddy currents have been studied in a ring shaped iron and nickel sample with rectangular cross-section of the ring. By applying a block-shaped magnetic field in the ring by a toroidal coil the magnetisation in the ring is reversing periodically in time, starting by domain nucleation at certain centres at the ring surface, which expand in time until they merge to a more or the less flat domain wall moving to the centre of the ring. From the time dependent Larmor precession of the polarisation around the local magnetisation the wall mobility of the flat wall could be determined [19, 21], from the depolarisation the time dependent flatness of the moving wall [19, 22]. In similar studies in thin FeNi soft magnetic films the repelling forces between expanding domain nuclei, approaching each other from the opposite surfaces could be demonstrated [23].

Magnetic Phase Transitions

Because of the sensitivity of the Larmor precession for small magnetic inductions ND has been applied to study the critical behaviour in pure Fe and Ni. It appeared possible to determine the critical exponents β and γ with very high accuracy close to the critical temperatures of Fe and Ni [24].

The first order phase transition of Austenite - Ferrite Steel is very important in heat treatments of steels. With ND it appears possible to determine from the mean Larmor precession angle the mean fraction of ferrite, because ferrite is ferromagnetic, and from the depolarisation the mean particle size of the ferrite particles transformed [25]. This method appears to achieve quite unique information about this phase transition.

Superconductors

By scanning a very narrow neutron beam through a superconductor in a magnetic field, detailed information can be obtained about the magnetic flux penetration into the superconductor [26]. By studying the time dependence of ND after applying a pulse or alternating field, the time dependence of the flux penetration can be followed on millisecond scale [27].

Temperature dependence of ND in high T superconductor YBACU.

As an illustration of the application of the depolarisation technique, experiments were carried out on a sintered $\text{YBa}_2\text{Cu}_3\text{O}_x$ sample of size $5.35 \times 20.55 \times 11 \text{ mm}^3$ with a grain size between 1 and $10 \mu\text{m}$. [20]. The sample positioned inside a coil is clamped between a magnetic short circuit to prevent emerging flux from the sample and coil to affect the polarization of the beam outside the sample. The whole is positioned in a cryostat. At low temperature (4K) a pulsed magnetic field of $\sim 0.7 \text{ T}$ with 0.1 ms duration was applied after which the depolarization matrix was measured with rising temperature. Fig.2 gives the results of the average magnetic induction components B_x , B_y and B_z and the correlation parameters α_{\perp} and α_{\parallel} which show the correlations in the magnetic components perpendicular and parallel to the applied field direction.

The different temperature dependence of α_{\perp} and α_{\parallel} is striking and is interpreted as follows. Direct after the field pulse the fluxlines are randomly directed in the half sphere with some remanence in the initial field direction, but in bundles of $\sim 20 \mu\text{m}$ sizes of the same order as the crystallite size. With increasing temperature the fluxlines start to stretch themselves in the average fluxline direction. Above 20 K all fluxlines are parallel but still inhomogeneously distributed. Above 40 K no measurable depolarization is present and the fluxlines are distributed homogeneously over the sample. Above this temperature the linear T dependence of $\langle B \rangle$ indicates a $(T-T_c)^{1/2}$ dependence of the fluxline spacing

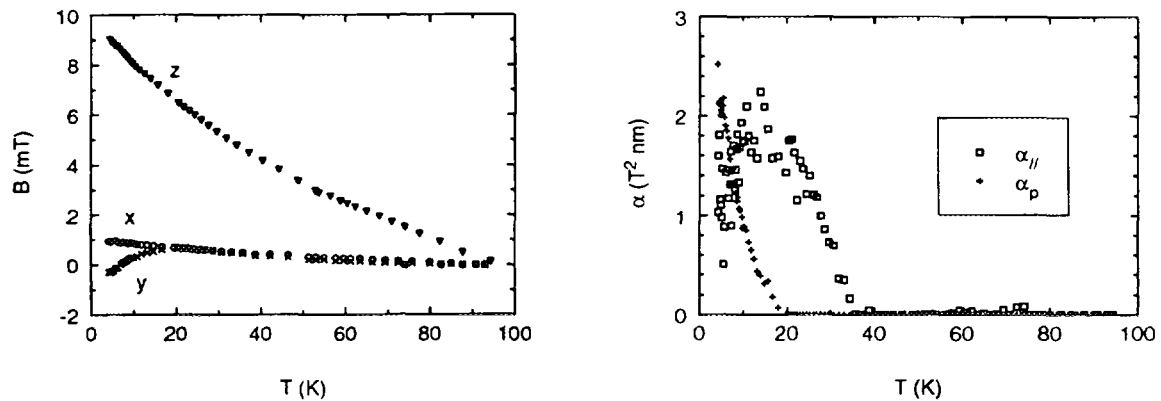


Fig.2 (Left) Remanent magnetic induction as a function of temperature, after zero-field cooling and a field pulse at 4.2 K. (Right) Average of the squared induction fluctuations perpendicular (α_{\perp}) and parallel (α_{\parallel}) to the initial applied field, plotted as a function of temperature.

Acknowledgements

The author wants to acknowledge W.H. Kraan, R. Rosman, P.T.Por, M. de Jong and W. Roest for their recent contribution in the presented work.

References

1. O.Halpern and T. Holstein, *Phys. Rev.* **59**, 960 (1941).
2. M. Burgy, D.J. Hughes, J.R. Wallace, R.B. Heller and W.E. Woolf, *Phys. Rev.* **80**, 953 (1950).
3. G.M. Drabkin, E.I. Zabidarov, Ya.A. Kasman, A.I. Okorokov and V.A. Trunov, *Sov. Phys. JETP* **20**, 1548 (1965);
4. A.I. Okorokov, V.V. Runov and A.G. Gukasov, *Nucl. Instr. and Methods* **157**, 487 (1978).

5. S.V. Maleyev, *J. de Physique* **43**, C7-23 (1982);
B.P. Toperverg and J. Weniger, *Z. Phys. B - Condensed Mater.* **74**, 105 (1989).
6. H. Rauch and E. Löffler, *Z. Physik* **210**, 265 (1968);
7. G. Badurek, G. Janeschitz, H. Weinfurter, J. Hammer, H. Rauch and W. Steiner, *J. de Physique* **43** C7-57 (1982);
A. Veider, G. Badurek, R. Groessinger and H. Kronmueller, *J. Magn. Magn. Mater.* **60**, 182 (1986)
8. M.Th. Rekveldt, *Textures and Microstructures* **11**, 127 (1989).
9. P.T. Por, M.Th. Rekveldt and W.H. Kraan, *Nucl. Instr. & Methods*, to be published 1995.
10. M. de Jong, J. Sietsma, M.Th. Rekveldt and A. van den Beukel, *Key Engineering Materials* **81-83**(1993)431.
11. Rosman, R. and M.Th. Rekveldt, *Z. Physik B: Condensed Matter* **79**, 61 (1990), and **81**, 149 (1990); *Thesis Delft*, 1991, ISBN 90-73861-02-0.
12. B.P. Toperverg and J. Weniger, *Z. Phys. B - Condensed Matter* **71**, 959 (1988)
13. B.P. Toperverg and J. Weniger, *Z. Phys. B - Condensed Matter* **74**, 105 (1989)
14. M. de Jong, B.P. Toperverg, J. Sietsma and M.Th. Rekveldt, to be published.
15. W.H. Kraan, M.Th. Rekveldt, K. Hemmes and J.C. Lodder, *IEEE Transactions on Magnetics*, **Mag-23**, 65 (1987).
W.H. Kraan, M.Th. Rekveldt, *Journ. de Physique, Colloq. C8, suppl. au no12*, 49 (1988) C8-1981
W.H. Kraan, M.Th. Rekveldt, P. de Haan, J.C. Lodder, *J. Magn. Magn. Mat.* 120 (1993) 372
W.H. Kraan, V.E. Mikhailova, M.Th. Rekveldt, *J. Magn. Magn. Mat.* 140-144 (1995) 1905
16. G.P. Felcher, R.O. Hilleke, R.K. Crawford, J. Haumann, R. Kleb and G. Ostrovski, *Rev. Sci. Instrumen.* **58**, 609 (1987).
17. K. Krezhov, V. Lillkov, P. Konstantinov and D. Korneev, *J. Phys.: Condens. Matter* **5** (1993) 9277
18. P.T. Por, W.H. Kraan, J. Mes, M.Th. Rekveldt, *Proc. of MRM'95, Oxford, UK* (1996)
19. F.J. van Schaik, J.W. Burgmeyer and M.Th. Rekveldt, *J. Appl. Phys.* **52**, 352 (1981).
F.J. van Schaik, M.Th. Rekveldt and J.W. van Dijk, *J. Appl. Phys.* **52**, 360 (1981).
20. W. Roest, M.Th. Rekveldt, *Phys. Rev. B*, **48**, (1993) 6420-6425; *Proc. 7th International Workshop on Critical Currents*, (World Scientific, Singapore, 1994) p.201.
21. N. Stüsser, M.Th. Rekveldt, *J. Appl. Phys.* 63(6), 1988, 2065
22. N. Stüsser, M.Th. Rekveldt, *J. Appl. Phys.* 61(9), 1987, 4579
23. M.Th. Rekveldt, H.J.L. van der Valk, *IEEE Trans. on Magn.*, Vol MAG-17.no.6, 2932.
24. N. Stusser, M.Th. Rekveldt, T. Spruijt, *Phys. Rev. B* 33 (1986) 6423
25. S.G.E. te Velhuis, M.Th. Rekveldt, S. van der Zwaag, *Ironmaking and Steelmaking* 1995 Vol.22 No.1 81
26. W. Roest, M.Th. Rekveldt *Physica C* 248 (1995) 213-221
W. Roest, M.Th. Rekveldt, *Physica C* 252 (1995) 264-274
27. W. Roest M.Th. Rekveldt, *Proc. 1994 Topical Intern. Cryogenic Materials Conf. Critical State in SC.* '94, oct. 24-26, 1994, Tokai Un. Pacific Center, Honolulu 24-26 oct. '94, Hawaii, ISBN 981-02-2248-3, pg. 157-164



SMALL ANGLE NEUTRON SCATTERING

B.A. DASANNACHARYA, P.S. GOYAL

Bhabha Atomic Research Centre,
Bombay, India

Abstract

Small angle neutron scattering (SANS) is one of the most popular neutron scattering technique both for the basic research and as a tool in the hands of applied scientist. SANS is used for studying the structure of a material on a length scale of 10 - 1000 Å. SANS is a diffraction experiment that involves scattering of a monochromatic beam of neutrons in order to obtain structural information about macromolecules and heterogeneities.

This paper will discuss the design of SANS spectrometers with a special emphasis on the instruments which are better suited for medium flux reactors. The design of several different types of SANS spectrometers will be given. The optimization procedures and appropriate modifications to suit the budget and the space will be discussed. As an example, the design of a SANS spectrometer at CIRUS reactor Trombay will be given.

1. Introduction

Small angle neutron scattering (SANS) is used for studying the structure of a material on a length scale of 10-1000 Å [1,2]. This is an excellent tool for obtaining structural information about macromolecules (biological molecules, polymers chains, colloid particles, micelles etc.) and heterogeneities like precipitates, microvoids and magnetic inhomogeneities in the material. In particular, SANS is used to study the sizes and shapes of 'particles' dispersed in a homogenous medium. In suitable cases, it also provides information about inter-particle interactions.

SANS is complementary to small angle X ray scattering (SAXS) and electron microscopy in certain problems of biology and metal physics. However, there is a wide field of applications which can only be studied using SANS, in particular problems of magnetism and certain experiments in colloid and polymeric science. SANS is being increasingly used by solid state physicists, chemists, metallurgists and biologists. The information obtained by this technique is often of direct interest to the industry.

SANS is a diffraction experiment that involves scattering of a monochromatic beam of neutrons (wave length λ), from the sample and measuring the scattered neutron intensity as a function of scattering angle Θ at small scattering angles. The typical wave vector transfer $Q (= 4 \pi \sin 1/2 \Theta/\lambda)$ in these experiments is $\sim 0.01 \text{ \AA}^{-1}$.

A variety of SANS spectrometers have been designed and built. Broadly speaking, they can be divided into three categories, namely, (i) conventional SANS spectrometers which use long flight paths and position sensitive detectors [3], (ii) Bonse-Hart type double crystal diffractometers [4] and (iii) the spectrometers based on photographic techniques where flight paths are kept small by using high resolution detectors (Gadolinium foil

followed by a X ray film) [5]. This report discusses the design aspects of above spectrometers with a special emphasis on the instruments which are suited for medium flux reactors.

2. Requirements of a SANS Spectrometer

The density distribution of the scattering object in real space is related the intensity distribution in Q space through a Fourier transform. The characteristic size R_0 in real space gives rise to an intensity distribution whose width is $\sim 2\pi/R_0$. Thus to examine a typical particle size of R_0 , one needs to do a scattering experiment that spans a Q range an order of magnitude on each side of the value $Q_0 = 2\pi/R_0$. This puts a demand on the SANS spectrometer to provide a minimum of Q ($= Q_{\min}$) and the step size δQ . In a detailed study of the particle surface area or the number density of particles, one has to often examine the Porod region ($Q R_0 \sim 20$) of the scattered profile also [2]. This puts a demand on the maximum accessible Q($=Q_{\max}$) range on the spectrometer.

In short, to study a particle size R_0 , one would like to have $Q_{\min} \sim 1/R_0$, $\delta Q \sim 1/5 R_0$ and $Q_{\max} \sim 20/R_0$. At times, it may not be possible to cover the full range of ($Q_{\max}-Q_{\min}$) in a step size of δQ . The spectrometer, having a provision to vary Q_{\max} or Q_{\min} depending on δQ is, therefore, highly desirable.

In addition to Q_{\min} , Q_{\max} and δQ , the other important parameter in designing a SANS spectrometer is the resolution ΔQ of the spectrometer. As we shall see later, ΔQ and Q_{\min} are intimately related. To improve ΔQ , one has to necessarily lower Q_{\min} and vice versa. The SANS spectrometers on medium flux reactors have typical values of $Q_{\min} = .005 \text{ \AA}^{-1}$, $\delta Q \sim .001 \text{ \AA}^{-1}$, $Q_{\max} = 0.2 \text{ \AA}^{-1}$ and $\Delta Q/Q \sim .10$ (say at $Q \sim .01 \text{ \AA}^{-1}$). This kind of instrument can be comfortably used to study a particle size of $\sim 200 \text{ \AA}$. In suitable cases, its capabilities can be extended up to $R_0 = 500 \text{ \AA}$

3. SANS Spectrometer Design

In principle, the requirements for SANS spectrometer are simple in comparison with other neutron instruments. A well-collimated, moderately monochromatic neutron beam is extracted from the neutron source by means of a monochromator and collimated using suitable apertures. The sample elastically scatters neutrons through small angles and the intensity as a function of scattering angle is detected and recorded by neutron detectors and data acquisition instrumentation downstream. Fig.1 gives a schematic representation of the essential features of a SANS system [3]. Neutrons escape the source volume with nearly a Maxwellian spectrum whose characteristic temperature depends on the moderator temperature T_m . A slice of this distribution is transmitted by the monochromatic system and enters an evacuated flight path L_1 with angular limits defined by the radii R_{ns} and R_s , which are source and sample apertures respectively. The direct and scattered beams pass through a second evacuated flight tube L_2 and impinge on the two dimensional detector plane. The flight tubes are evacuated to eliminate air scattering which would produce an effective degradation of 5-10% per meter, depending on the neutron wavelength. A carefully dimensioned beam stop masks the detector from the total direct beam.

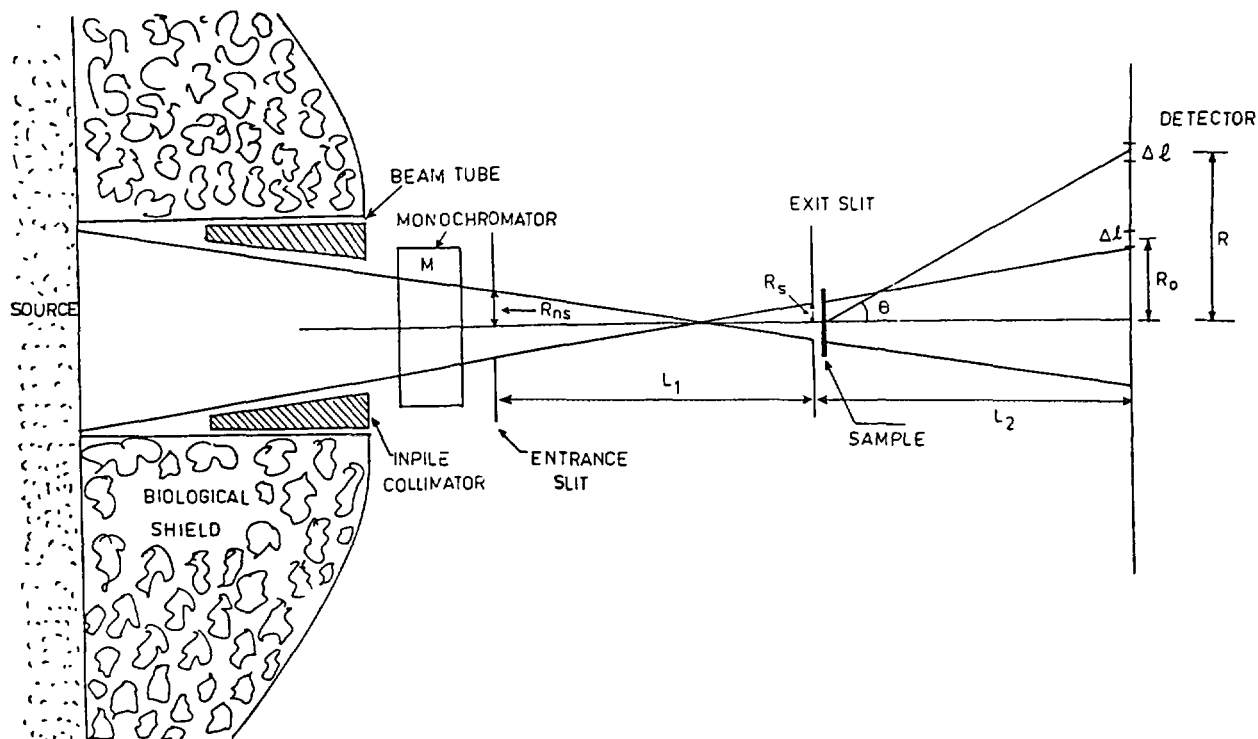


FIG. 1. Schematic representation of a SANS spectrometer.

At small scattering angles, Q corresponding to a scattering angle Θ is given by

$$Q = \frac{2\pi}{\lambda} \Theta \quad (1)$$

Small angle scattering occurs close to the incident beam. The presence of fast neutrons and γ -rays in the direct beam makes these experiments difficult. The use of curved guides is recommended as it takes the neutron beam away from the direct sight and thereby reduces the background.

Further, it follows from Eq. (1) that the scattering angle is proportional to the wavelength for a given Q (say = Q_{\min}). Thus the longer the wavelength the better defined is the angle, and possibly the closer one can get to the main beam. SANS machines use 4-10 Å neutrons. The Maxwellian spectrum of neutrons in a reactor ($T_m \sim 350$ K) usually have very low intensities in the above wavelength range. Thus use of a cold neutron source ($T_m \sim 50$ K) is desirable as it shifts the Maxwellian spectrum to larger wavelength region, thereby increasing the useful flux several folds.

Though, in principle, it is not necessary to have a two dimensional position sensitive detector for azimuthally isotropic scatterers, the use of such a detector substantially improves the data collection efficiency by recording the data over the full annular ring corresponding to the scattering angle Θ . The x-y detector, however, becomes necessary for investigating the anisotropy in scattering in the azimuthal plane.

The cold neutron source, neutron guides and x-y detectors, though expensive, are now extensively used. These are especially useful for medium flux reactors, where incident neutron intensities are small. The Q range on the above spectrometer can be varied by any of the following three methods: (i) varying the wavelength of incident neutrons, (ii) varying the distance L_2 between the sample and the detector or (iii) rotating the detector arm about the sample position. To cover the Guiner and Porod regions of the scattered profile, it is desirable that the spectrometer has a possibility of varying Q range.

4. Optimisation of a Conventional SANS Spectrometer

We assume that slits R_{ns} and R_s are so designed that sample sees the full neutron source. In that case, L_1 in Fig.1 is taken as a distance between the source and the sample. The detector has a pixel size of $\Delta l \times \Delta l$. Neutrons counted in n^{th} cell thus correspond to a scattering angle of $\Theta = n\Delta l/L_2$. The expressions for various parameters of a SANS machine can thus be written as

$$Q = \frac{2\pi}{\lambda} \frac{n\Delta l}{L_2} \quad (2)$$

$$\delta Q = \frac{2\pi}{\lambda} \frac{\Delta l}{L_2} \quad (3)$$

$$Q_{\min} = \frac{2\pi}{\lambda} \left(\frac{R_{ns} + R_s}{L_1} + \frac{R_s + \Delta l}{L_2} \right) \quad (4)$$

It is assumed that useful data are obtained from those pixels which are at least one pixel away from the extreme radius of the direct beam profile at the detector plane. It is seen that Q_{\min} depends on the sample size R_s . To obtain low values of Q_{\min} , one has to necessarily use small samples. If n_0 is the outermost pixel on the detector, maximum accessible Q is given by

$$Q_{\max} = \frac{2\pi}{\lambda} \frac{n_0 \Delta l}{L_2} \quad (5)$$

The neutrons reaching n^{th} pixel (mean scattering angle Θ) could have a range of scattering angles depending on the apertures R_{ns} and R_s . It is believed that the scattering angles will have Gaussian distributions with a mean angle Θ . The spread $\Delta\Theta$ in Θ is given by [6]

$$\Delta\Theta = \sqrt{2 \ln 2} \left[\left(\frac{R_{ns}}{L_1} \right)^2 + R_s^2 \left(\frac{1}{L_1} + \frac{1}{L_2} \right)^2 + \frac{1}{3} \left(\frac{n\Delta l}{L_2} \right)^2 \right]^{1/2} \quad (6)$$

The resolution of the instrument is given by

$$\frac{\Delta\Theta}{Q} = \left[\left(\frac{\Delta\lambda}{\lambda} \right)^2 + \left(\frac{\Delta\Theta}{\Theta} \right)^2 \right]^{1/2} \quad (7)$$

where $\Delta\lambda$ is the spread in the incident neutron wavelength.

Now coming to the intensities, the total number of incident neutrons per sec at the sample is given by

$$\Phi_s = \frac{1}{4\pi} \Phi_o (\pi R_{ns})^2 \frac{\pi R_s^2}{L_1^2} \quad (8)$$

Where Φ_o n/cm²/sec is the reactor flux at the beam-entrance. If $d\Sigma/d\Omega$ is the scattering cross-section per unit volume of the sample, then the scattered neutron intensity detected in a pixel of area $\Delta l \times \Delta l$ at detector is given by

$$C_D = \Phi_s t T_s \frac{d\Sigma}{d\Omega} \cdot \frac{\Delta l x \Delta l}{L_2^2} \cdot \eta \quad (9)$$

Where t is sample thickness, T_s sample transmission and η is the detector efficiency. That is,

$$C_D = \left(\frac{1}{4\pi} \Phi_o \pi^2 t T_s \eta \frac{d\Sigma}{d\Omega} \right) \left(\frac{R_{ns} R_s \Delta l}{L_1 L_2} \right)^2 = C_o \left(\frac{R_{ns} R_s \Delta l}{L_1 L_2} \right)^2 \quad (10)$$

where C_o is a constant. We note that the characteristic parameters Q_{\min} , δQ , Q_{\max} , ΔQ and C_D depend on five geometrical parameters namely R_{ns} , R_s , Δl , L_1 and L_2 . The optimization involves finding the relations between above parameters so that one gets maximum count rate C_D for a given angular spread $\Delta\Theta$.

It can be shown that the required condition is

$$L_1 = L_2 \text{ and } R_{ns} = 2R_s = \Delta l \quad (11)$$

Most of the spectrometers choose $L_1 = L_2$. Ideally, this optimization should be followed when the detector is moved forward to increase the range of Q_{\max} . Under condition (11), we note that

$$C_D \sim (\Delta l)^2 (R_s/L_1)^4 \quad (12)$$

That is,

$$C_D \sim (\Delta\Theta_i)^4 \quad (13)$$

where $\Delta\Theta_i$ is the incident beam divergence and decides Q_{\min} . Resolution ΔQ also depends on $\Delta\Theta_i$. We note that if one tries to improve Q_{\min} or ΔQ , one ends up paying an heavy price in the intensity because of fourth power variation in Eq.(13). This is because of the fact that Q_{\min} is dependent on the sample size. However, if one can decouple the incident beam divergence (as is the case with double crystal diffractometers), it is possible to use bigger samples.

Typically, a SANS spectrometer has $L_1 = L_2 = 5$ m, $\lambda = 6$ Å, $R_{ns} = 2$ cm, $R_s = 1$ cm and a 64 cm x 64 cm detector with $\Delta l = 1$ cm. This will have :

$$\begin{aligned}
 \delta Q &= .002 \text{ \AA}^{-1} \\
 Q_{\min} &= .01 \text{ \AA}^{-1} \\
 Q_{\max} &= 0.067 \text{ for } L_2 = 5 \text{ m} \\
 &= 0.167 \text{ for } L_2 = 2 \text{ m} \\
 \Delta\Theta &= 5.77 \times 10^{-3} \text{ radians}
 \end{aligned} \tag{15}$$

That is, typically $\Delta\Theta/\Theta$ will vary from about 0.58 to 0.10 as one moves from the edge of the direct beam profile at the detector to the outer edge of the detector. It is because of this that one does not need very good wave length resolution in a SANS spectrometer; Eq.(7) suggests that $\Delta Q/Q$ will be mainly decided by $\Delta\Theta/\Theta$ especially at low Q .

5. Most Commonly Used SANS Spectrometer

SANS spectrometer at high flux reactor at ILL is a prototype of a conventional SANS spectrometer [3]. It uses a beam from the cold neutron source and is installed on a curved guide. It uses $L_1=L_2$ and the entrance aperture is double the size of the sample aperture. L_1 can have a value up to 40m. The monochromator is the mechanical velocity selector. As already mentioned, SANS machines use moderately monochromatic beam. The typical wavelength resolution is ~ 0.10 . The mean wavelength is in range of 4 Å - 10 Å.

The incident neutron wavelength can be varied by varying the rotational speed of the velocity selector. The detector is a two dimensional position sensitive gas detector (64 cm X 64 cm). Q_{\max} of the instrument can be varied by moving the detector along the beam. A number of spectrometers using somewhat similar design are now operating in different laboratories in the world.

6. Possible Modifications to Conventional SANS Spectrometers

The SANS spectrometer of the type described above is very expensive and requires large space. At times, one has to make compromise with the performance of the instrument to cut down the cost and the convenience of fabrication and maintenance. The following are some of the modifications which could be considered depending on the budget or other constraints:

6.1 Monochromator

The following is a list of monochromators which could be used in place of a velocity selector on a SANS machine :

(a) Pairs of double crystal monochromators

In a double crystal monochromator, neutron beam is reflected by two crystals, which are kept parallel to each other and are separated by a distance. The wavelength spread obtained by a single pair of crystals is usually quite small. This can be spoiled by using several pairs of crystals which are misaligned ($\sim 0.5^\circ$) with respect to each other. Such systems have been used [7] and have the advantage that the monochromatic beam is displaced from the incident beam and is therefore free from fast neutrons and γ ray backgrounds.

(b) Several misaligned crystals in a dog-leg configuration

The effective mosaic spread of a single crystal monochromator can also be spoiled by choosing the monochromator that consists of a number of crystals which are misaligned with respect to each other. The composite crystal system is designed to have an anisotropic effective mosaic spread. It is desirable that the system provides poor mosaic spread in the scattering plane without spoiling the mosaic in the direction perpendicular to the scattering plane. SANS spectrometer at Missouri Research Reactor uses such a monochromator [8].

(c) Filters such as BeO

BeO has a Bragg cut off wave length of 4.7 \AA . Thus when a reactor beam passes through block of BeO ($\sim 20 \text{ cm}$ long), BeO scatters off all those neutrons which have a wavelength spread of about 25% with a mean wave length at 5.2 \AA . As such, such an arrangement can be used for a SANS experiment [9]. The main drawback of this system is that the wave length distribution of the incident beam is not symmetric; in particular it has a long tail extending up to 10 \AA . It is, however, possible to reflect off large wave length neutrons (say $> 7 \text{ \AA}$) by using silicon wafers which are kept at required angle ($\sim 0.5^\circ$) to the incident beam.

6.2. Focusing Devices

It is possible to use an arrangement of slits such that several beams are incident on the sample; all these beams are focused on the detector centre and allow use of a bigger sample. This type of focusing collimators have been used on the SANS spectrometer at NIST [10].

The toroidal mirrors can also be used to focus the source on the centre of the detector [4]. This way instrument length can be considerably reduced without spoiling the instrument resolution.

The development of neutron lenses [11] could also be exploited to make low resolution SANS machines if one uses image plate detectors [12].

7. SANS Spectrometer at CIRUS Reactor Trombay

As an example of a simple SANS spectrometer on a medium flux reactor, in the following, we give a brief description of the spectrometer on Cirus reactor at Trombay. Cirus reactor provides a flux of 6×10^{13} n/cm²/sec at its full power of 40 MW. It does not have a cold source. SANS spectrometer has been operating on beam hole E13 of the above reactor for the last ten years. Fig. 2 gives the schematic drawing of the spectrometer. 10 cm dia beam from reactor is reduced to 1.0×1.5 cm² beam at sample position by using inpile collimator and slits S_1 and S_2 outside the biological shield. The collimator design and the apertures are chosen to obtain an angular divergence of $\pm 0.5^\circ$. The beam from the reactor passes through a single crystal of bismuth (10 cm long) and a polycrystalline block of beryllium oxide (20 cm long) before reaching the sample. Bi is used to remove γ rays. BeO, having a Bragg cut off wave length $\lambda_c = 4.7 \text{ \AA}$ serves the purpose of a monochromator. The wave length distribution $I(\lambda)$ vs λ of the filtered beam as measured using mica crystal is somewhat asymmetric in shape. It has a centre of gravity at 5.2 \AA with a full width at half maximum of $\pm 0.5 \text{ \AA}$. The incident neutron flux at sample position is 2×10^4 n/cm²/sec. The angular distribution of the scattered neutrons is measured using one dimensional position sensitive detector. The distance between the sample and the detector is 180 cm. The accessible Q range on above instrument is from 0.02 \AA^{-1} to 32 \AA^{-1} .

It is noted that a spectrometer of the type described above is easy to build. Further we find that inspite of the low flux, the Cirus machine has been successfully used for SANS studies. The scattering cross-section of up to 0.5 cm^{-1} can be easily measured. The above spectrometer is regularly used by BARC scientists and the university researchers. In particular, structural aspects and inter-micellar interactions in several micellar solutions have been studied [13-15]. Structures of some ferrofluids have also been investigated [16,17].

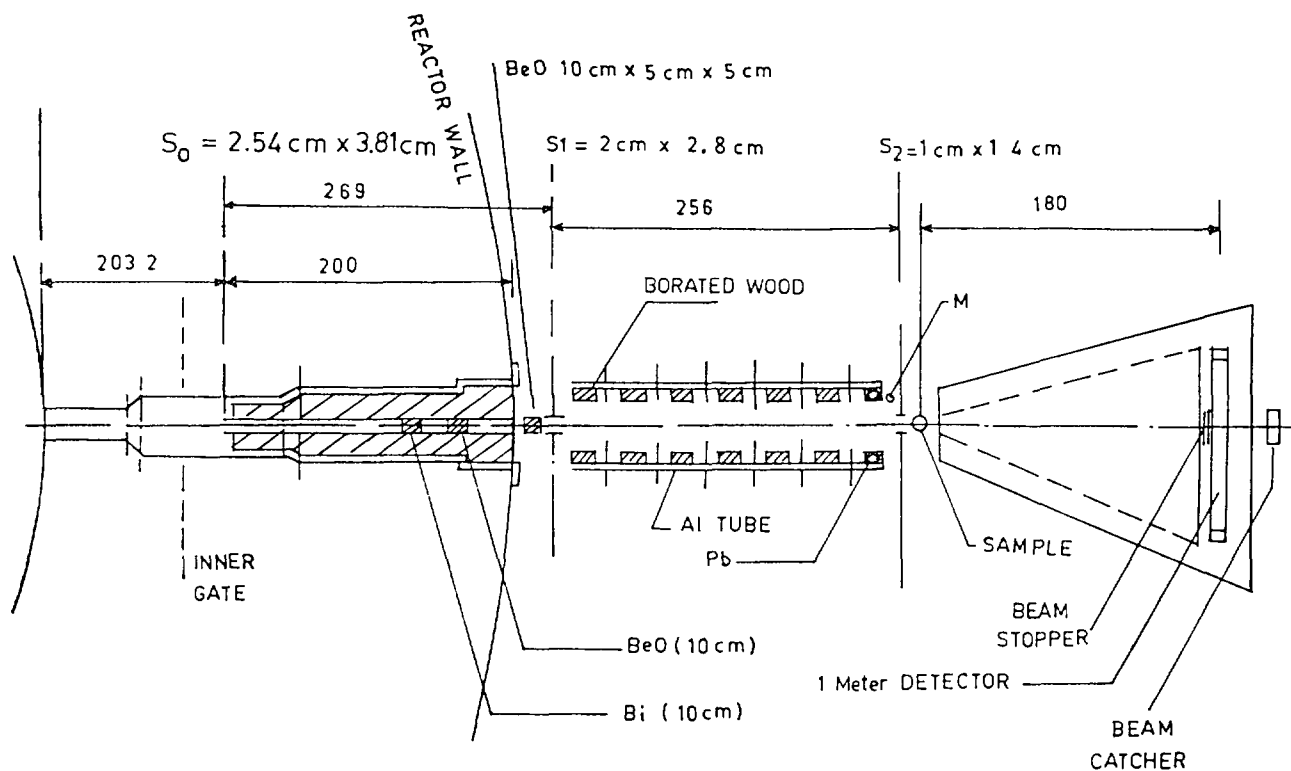


FIG. 2. Layout of the SANS spectrometer at the Cirus reactor, Bombay.

8. Different Types of SANS Spectrometers

The most commonly used SANS spectrometer has been described above. In the following, we give some other designs, which have also been used for SANS experiments.

8.1 Photographic Method for SANS

The experimental arrangement used in the photographic method [5] is similar to a conventional [3] position-sensitive detector based SANS spectrometer. The only difference is that the gas filled PSD in conventional machine is replaced by a gadolinium foil/ film converter. The high resolution ($\sim 100 \mu\text{m}$) of the foil-film combination for neutron detection allows a considerable reduction in the sample to detector distance. This arrangement allows the imaging of the scattered neutron distribution on a radiograph, which is then scanned using a microdensitometer.

The photographic method of SANS experiments has been tried at Dido reactor Harwell. The merit of this instrument lies in its small size and thus a lower cost. The main disadvantage is that to get a discernible density on the developed film, it is necessary to achieve a neutron exposure > 10 neutrons/ cm^2 . This makes it a very inefficient machine and that is perhaps the reason that this method did not become popular. The use of image plate detectors or charge coupled devices might improve the situation.

8.2 Double crystal diffractometers

The double crystal diffractometer makes use of Bonse - Hart's method for SANS experiments and is ideally suited for ultra low Q values (10^{-5} to 10^{-3} \AA^{-1}) [4]. The set up consists of two nearly perfect silicon crystals, which are aligned in the parallel configuration. The neutron beam from the reactor reaches the detector after undergoing two Bragg reflections from the two crystals. The sample is kept between the two crystals. SANS experiment involves recording the rocking curve of the 2nd crystal with and without sample. The changes in the rocking curve can be used to extract the SANS distribution of the sample. This type of SANS machine can be fruitfully used even on the modest flux reactors.

The wings of the rocking curve in the above experiment usually have significant contribution from diffuse background and this puts a restriction on the maximum Q range of the instrument. Use of channel cut Si crystals in place of ordinary ones is recommended since it reduces the diffuse background [18]. The other possibility is to use the bent crystals. The bent crystal, because of increased effective mosaic, provides higher intensity without much increase in the background [19].

9. Summary

SANS is one of the most popular neutron scattering technique both for the basic research and as a tool in the hands of applied scientist. It is often seen that SANS instruments are installed on cold source beam lines and use two dimensional position sensitive detectors. This is certainly highly desirable but also expensive. There are a large class of experiments however, which can be done on somewhat simpler machines.

This paper discusses the design aspects of SANS spectrometers with a special emphasis on the instruments which are better suited for medium flux reactors. The designs of several different types of SANS spectrometers have been given. The optimization procedures and appropriate modifications to suit the budget and the space have been discussed. As an example, the design of a SANS spectrometer at CIRUS reactor Trombay is given.

References

1. C.G. Windsor, *J. Appl. Cryst.* 21, 582 (1988).
2. G. Kostorz in "Treatise on Materials Science and Technology" (ed.) G. Kostorz, Vol.15 (Academic Press, New York, 1979).
3. W. Schmatz, T. Springer, J. Scelten and K. Ibel, *J. Appl. Cryst.* 7, 96 (1974).
4. B. Alefeld, D. Schwahn and T. Springer, *Nucl. Inst. Meth. A* 274, 210 (1989).
5. A.J. Allen and D.K. Ross, *Nucl. Inst. Meth.* 186, 621 (1981).
6. C.G. Windsor, "Pulsed Neutron Scattering" (Taylor and Francis Press, London, 1981).
7. H.R. Child and S. Spooner, *J. Appl. Cryst.* 13, 259 (1980).
8. D.F.R. Mildner, R. Berliner, O.A. Pringle and J.S. King, *J. Appl. Cryst.* 14, 370 (1981).
9. J.A.E. Desa, S. Mazumdar, A. Sequiera and B.A. Dasannacharya, *Solid State Physics (India)* C28, 318 (1985).
10. C.J. Glinka, J.M. Rowe and J.G. LaRock, *J. Appl. Cryst.* 19, 427 (1986).
11. Q.F. Xiao, H. Chen, D.F.R. Mildner, R.G. Downing and R.E. Benenson, *Rev. Sci. Inst.* 64, 3252 (1993).
12. F. Ne, D. Gazeau, J. Lambard, P. Lesieur, T. Zemb and A. Gabriel, *J. Appl. Cryst.* 26, 763 (1993).
13. P.S. Goyal, S.V.G. Menon, B.A. Dasannacharya and V. Rajagopalan, *Chem. Phys. Lett.* 211, 559 (1993).
14. V.K. Aswal, P.S. Goyal, S.V.G. Menon and B.A. Dasannacharya, *Physica B* 213, 607 (1995).
15. K.S. Rao, P.S. Goyal, B.A. Dasannacharya, V.K. Kelkar, C. Manohar and S.V.G. Menon, *Pramana- J. Phys.* 37, 331 (1991).

16. R.V. Mehta, R.V. Upadhyay, B.A. Dasannacharya, P.S. Goyal and K.S. Rao, J. Magnetism and Mag. Mat. 132, 154 (1994).
17. R.V. Mehta, P.S. Goyal, B. A. Dasannacharya, R.V. Upadhyay, V.K. Aswal and S.M. Sutaria, J. Magnetism and Mag. Mat. 149, 47 (1995).
18. D. Schwahn, A. Miksowsky, H. Rauch, E. Siedl and G. Zugareck, Nucl. Inst. Meth. A 239, 229 (1985).
19. J. Kulda and P. Mukula, J. Appl. . Cryst. 16, 498 (1983).

**NEXT PAGE(S)
left BLANK**



B. FARAGO

Institute Max van Laue–Paul Langevin,
Grenoble, France

Abstract

Until 1974 inelastic neutron scattering consisted of producing by some means a neutron beam of known speed and measuring the speed of the neutrons after the scattering event. The smaller the energy change was, the better the neutron speed had to be defined. As the neutrons come from the reactor with an approximately Maxwell distribution, an infinitely good energy resolution can be achieved only at the expense of infinitely low count rate. This is not very practical.

In 1972 F. Mezei discovered the method of Neutron Spin Echo. As we will see in the following this method decouples the energy resolution from intensity loss and allows high resolution inelastic measurements even at low, medium flux reactors.

Basics

Theory

It can be shown [1] that an ensemble of polarized particle with a magnetic moment and 1/2 spin behaves exactly like a classical magnetic moment. Entering a region with a magnetic field perpendicular to its magnetic moment it will undergo Larmor precession. In the case of neutrons:

$$\omega = \gamma \cdot B$$

where B is the magnetic field, ω is the frequency of rotation and $\gamma=2.916\text{kHz/Oe}$ is the gyromagnetic ratio of the neutron..

Now let us consider a polarized neutron beam which enters a B_1 magnetic field region of length l_1 . The total precession angle of the neutron will be:

$$\varphi_1 = \frac{\gamma B_1 l_1}{v_1}$$

depending on the velocity (wavelength) of the neutrons. If v has a finite distribution (eg 15%) after a short distance (a few turns of the polarisation) the beam will appear to be completely depolarised. If now the beam will go through an other region with opposite field B_2 and length l_2 the total precession angle

$$\varphi_{\text{tot}} = \frac{\gamma B_1 l_1}{v_1} - \frac{\gamma B_2 l_2}{v_2}$$

In the case of elastic scattering (or no scattering) on the sample $v_1=v_2$ and if $H_1 l_1 = H_2 l_2$ φ_{tot} will be zero independently of v and we recover the original beam

polarisation. Let us suppose now that the a neutron was scattered with a small ω energy exchange between the H_1 and H_2 region. In that case

$$\varphi_{\text{tot}} = \frac{\gamma B l}{2mv} \omega$$

where m is the mass of the neutron

If we put an analyser after the second precession field the probability that a neutron is transmitted is

$$\langle \cos \varphi \rangle$$

We have to take the expectation value of $\langle \cos \rangle$ over all the scattered neutrons. At a given q the probability of the scattering with ω energy exchange is by definition $S(q, \omega)$. Consequently the beam polarisation measured

$$\langle \cos \varphi \rangle = \frac{\int \cos\left(\frac{\gamma B l}{2mv} \omega\right) S(q, \omega) d\omega}{\int S(q, \omega) d\omega} = S(q, t)$$

So NSE directly measures the intermediate scattering function.

Implementation

In practice reversing the magnetic field is difficult as at the boundary between them around the zero field point the beam gets easily depolarised. Instead a continuous horizontal field is used (conveniently produced by solenoids) and a $\pi/2$ flipper starts the precession by flipping the horizontal polarization perpendicular to the magnetic field. The field reversal is replaced by a π flipper which reverses the precession plane around an axis and at the end a second $\pi/2$ flipper stops the precession and turns the recovered polarisation in the direction of the analyser. We will come to a little more detailed explanation of the technics in the check-list section.

Variants

Inelastic NSE

One could ask the question whether the method could be used in the case of finite energy exchange? The answer is yes, but with some modification. By choosing $H_1 l_1 \neq H_2 l_2$ the same Fourier back-transformation happens but around [1]:

$$\omega = \frac{m}{2\hbar} v_1^2 \left(1 - \left(\frac{B_1 l_1}{B_2 l_2} \right)^{3/2} \right)$$

v_1 is the velocity of the incoming neutron and the scattering is supposed to be downscattering in energy.

The problem here is that around $\omega=0$ $S(q,\omega)$ has always a strong peak (either quasielastic scattering, diffuse elastic scattering and/or incoherent scattering) In reality we should not speak about a fix q but rather a fix scattering angle. This however does not change the fact that there is a lot of unwanted scattering. The solution is to use a triple axis spectrometer geometry which acts as a filter, pre-cutting an interval around ω_0 with a coarse resolution compared to NSE. As triple axis spectroscopy with polarized neutrons already in itself is very poor in intensity, if on the top we want to put an NSE, this is certainly not something we would recommend at a medium size reactor, at least at the present state of reflectivity of polarizing (analysing) monochromators. The interested reader should refer to [1].

Magnetic scattering

The application of NSE to magnetic scattering has only two special features.

One is that ferromagnetic samples hardly can be studied. The random orientation of manetic domains introduces Larmor precessions around random axis and unknown precession angles normaly resulting in depolarisation of the beam and the loss of the echo signal. In some cases the application of a strong external field to aligne all the domains in the same direction can help for one component of the polarisation to survive [1]

The second is the case of paramagnetic scattering. There the spin components in the sample perpendicular to q which give the magnetic scattering. As the precession plane of the neutrons in the usual NSE geometry is perpendicular to that one, the neutrons which are scattered spin paralell q will undergo spin flip scattering, while those arriving with q perpendicular q will have 50% probability of spin flip and 50% probability of non spin flip scattering. Accordingly the scattered beam polarisation can be decomposed as

$$\frac{1}{2} \begin{pmatrix} P_x \\ P_y \\ P_z \end{pmatrix} + \frac{1}{2} \begin{pmatrix} -P_x \\ P_y \\ P_z \end{pmatrix}$$

(The precession plane being x,y)

We can realise that the second term is equivalent to a π flipped beam around the y axis. Consequently without a π flipper the second term will give an echo with 50% amplitude of the magnetic scattering, while using a π flipper the first term results in an echo of 50% amplitude plus a full echo from the eventual nuclear scattering as well. This means that without π flipper ONLY the magnetic scattering gives an echo signal, which eliminates the need of time consuming bacground measurements to separate the nuclear contribution.

ZFNSE

This method was introduced by Gähler & Golub [2]. We will just give a quick explanation how to understand the basic principle. The method has clear advantages in the case of Inelastic NSE. Whether the quasielastic NSE will or will not have better performance we will see when sufficient experience will be accumulated with ZFNSE.

The magnetic field profile along the axis of a classical NSE schematically is the following: Nearly zero horizontal field at the first $\pi/2$ flipper, strong (H_0) field in the first solenoid, nearly zero at the π flipper, again strong field in the second precession region, finally nearly zero again at the second $\pi/2$ flipper. In H_0 the neutron precesses with the Larmor frequency $\omega_0 = \gamma H_0$. Let us choose now a rotating frame reference which rotates with ω_0 . In this frame the neutron seems not to precess in the solenoids which means it sees $H'_0 = 0$. However now in the originally low field region it will rotate with ω_0 which indicates the presence of a strong H_0 field. Our static flippers' small field will appear to rotate also with ω_0 . Let us realise this configuration now in the lab frame. Inside the π and $\pi/2$ flippers we must have a strong static field H_0 and perpendicular to that a small field which rotates with $\omega_0 = \gamma H_0$. This best realized with a flat solenoid like winding of a relatively thick Al ribbon to create a strong magnetic field perpendicular to the neutron beam and inside a smaller coil perpendicular both to the neutron beam and to the strong field. This coil we have to connect to a radiofrequency generator which will produce the necessary rotating field. In between the these flippers a strictly zero field region has to be insured to avoid "spurious" spin precession. The first prototype spectrometers all use mu-metal shielding + earth field compensation.

Multidetector variants

At the time of writing three instruments are experimented to to extend the "classical" NSE to use multidetectors, and thus reducing the data acquisition time. In all cases the problem is that one can collect useful information in all detectors only if the echo condition can be fulfilled simultaneously for all of them. This is not a straightforward exercise as the field integrals must be equal with a precision of 10^{-5} !

a) The most straightforward is applied on the instrument IN15 at the ILL. Here simply the solenoid diameters were increased to allow the use of a small 32cm x 32cm multidetector. The difficulty is to make a sufficiently big Fresnel coil with the necessary precision without absorbing a substantial fraction of the neutron beam.

b) On In11 an option is being constructed to replace the secondary solenoid with a camamber shaped sector magnet. The expected field homogeneity will be inherently lower, but in many cases in the high q region the best possible resolution is not needed but the scattered intensity is relatively low.

c) In Berlin a totally new approach was initiated by F. Mezei. If one takes a Helmholtz like coil, but the two half generates a field opposite to each other than in the equatorial plane the field is guaranteed to be rotationally symmetric. The neutron beam comes in along a radius and the detectors are placed all around. The practical problem here is a zero field point at the sample position which would depolarize the beam. The solution proposed is to deplace this zero point above the sample with the help of some additional coils.

Check List:

Here we will give list of points which we consider crucial to the best possible implementation of a NSE spectrometer, furthermore a few usefull hints:

1. Neutron beam:

Usually little choice is offered here and it is mainly determined by the reactor characteristics. Nevertheless to have the best possible flexibility in the choice of the used wavelength and to facilitate the beam polarisation a guide end position is the best place. (For an example what can be gained with variable wavelength see examples at the end) In any case as the resolution increases with λ^3 , a cold neutron beam is needed for high resolution studies. At present there is no NSE spectrometer installed on a thermal beam. It would have a limited resolution but at the relatively high q values that it could reach, there might be no need for extreme resolutions. In the following we suppose a cold neutron beam.

2. Monochromatisation:

NSE can tolerate in most cases a broad wavelength distribution. eg 15% FWHM. A neutron velocity selector with high transmission is the best choice.

3. Polariser:

Very essential part of the spectrometer. Generally supermirrors are used. There are two possible choice. Reflection or transmission mode. As in general the polariser-sample distance is in the order of 2-3m the main danger in both cases is the unwanted increase of the incoming beam divergence on the polariser. Due to the relatively big distance here one can loose integer factors in the neutron flux on the sample. Inherently the reflecting supermirrors are more susceptible to increase the beam divergence, and also have the inconvenience that the reflection angle might have to be adjusted to different wavelength if the usefull range is large enough. On the other hand the supermirrors of this type were easier to obtain.

Recent progress allowed the production of supermirrors on Si wafers with sufficiently good quality to make quavity like transmission devices see Fig 1 The smaller the angle of the V form Si plates the shorter wavelength can be used. In principle they could be fairly broad band devices, but at long wavelength they suffer from absorption in the Si plates and also the first tests show a certain hole around zero angle in the divergence. As this is the most important part of the incoming beam it needs a closer examination. If we look on Fig 1 the trajectory A which comes parallel with the beam axis becomes very divergent after the polariser

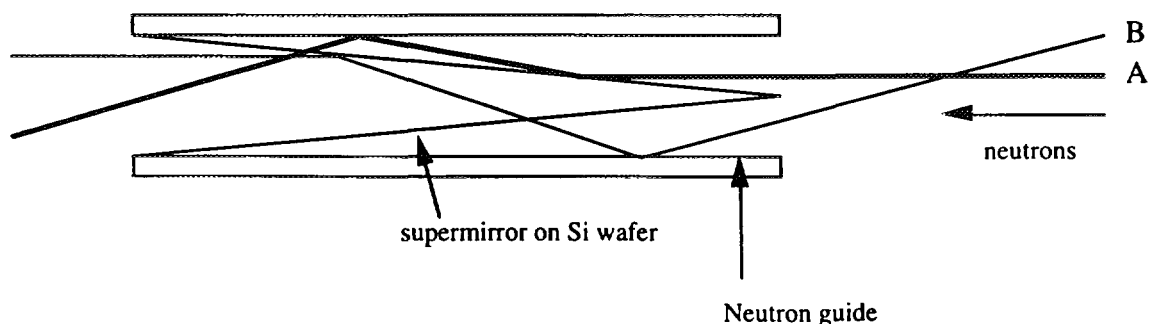


Fig. 1.

if the wavelength is sufficiently large that the first reflection is below the critical angle even for neutrons with the good spin. Thanks to Liouville however there is trajectory **B** which arrives with a large divergence and as shown on Fig 1 will go out of the polariser parallel with the axis. However, if before the polariser due to misalignment or cuts in the guide, this very divergen neutron is missing, trajctory **A** will not be replaced and effectively the center of the beam will be emptied.

$\pi/2$ flipper:

For the flipper itself use the same construction as in ref [1] page 35 fig. 12 with the only difference that simple naked Al wire works as well as the enameled of, if not winded too tightly and using an isolating frame. On the other hand the transmission of 8Å increases by 5-7% which means 15-21% gain in intensity because of the three flippers. The $\pi/2$ flipper needs a given vertical field inside the flipper and constant horizontal component of the field through the flipper. As inside due to the neighboring precession magnet the field changes as we measure at different Fourier times, this variation needs to be compensated. If the field to be compensated is small a simple ring like coil around the flipper is sufficient. If the fields are important than one might need a Helmholtz arrangement, but the two coils driven with different currents. The explanation is the following: as the field in the precession solenoid is changing during the measurement, and the field in the polariser stays constant, the minimum point is deplaced as the precession field changes. We can not constantly displace the $\pi/2$ flipper to this minimum, but than in some cases with a single compensation coil we might create a zero field point before decreasing the horizontal field to the desired value on the flipper. This would depolarize the beam and kill the echo signal. With the asymmetric Helmholtz configuration the slope of the compensating field can be matched to the slope of the stray fields and thus avoiding this problem.

π flipper:

Nearly identical to the $\pi/2$ flipper with the exception that the horizontal field has to be decreased practically to zero. On In11 the pi flipper is sufficiently far from the precession solenoids so a simple coil around the flipper is enough to have $\approx 95\%$ efficiency.

“Fresnel coils”

The solenoids produce inherently slightly inhomogeneous field integrals for finite size beams. Let us consider the field integral difference between the trajectory on the symmetry axis and a parallel one at a distance r. In leading order this gives:

$$\Delta \int H dz \cong \frac{r^2}{8} \int \frac{1}{H(z)} \left(\frac{\partial H(z)}{\partial z} \right)^2 dz$$

It can be shown also that a current loop placed in a strong field region changes the field integral by $4\pi I$ if the trajectory passes inside the loop at by zero if it passes

outside. To correct the above calculated r^2 dependence we just have to place properly arranged current loops in the beam. The so called Fresnel coils just do that.[1] They are usually made by printed circuit technology preparing two spirals where the radius changes with $r \approx \sqrt{\phi}$ placed back to back with a thinnest possible isolator (25micron kapton) to minimize neutron absorption.

Precession solenoids

From the experience on the IN11 spectrometer we know that the precise winding of the solenoids is essential. In '95 we have replaced the solenoids with a more precise ones and we have gained nearly a factor two in resolution! This gain came from the fact that a) the winding is made now on a solid Al tube which ensures very concentric geometry. b) an even number of winding layers avoids that there is a net current flow from one end of the solenoid to the other. c) The use of hollow copper conductor, to remove the resistive heating decreases thermal expansion d) special attention was paid to make the current connections in such a way that it does not create spurious magnetic field (at the coil ends the field decreases fast and the homogeneity is more sensitive to perturbative fields.

Also the power supplies, even if the the solenoids are in series and as such less sensitive to slow drifts, need to have a stability of 10^{-4} .

General points:

Especially at medium flux reactors where the experiments are rather slow, the mechanical and electrical stability of the experimental setup is a key point. When measuring 10^{-5} relative energy exchanges thermal expansion, or little displacement of the coils can falsify the measurements.

As many as possible power supplies should be used in a compensated way (driving the corresponding coils in the first and second half of the spectrometer) to eliminate eventual slow drifts. Even than $f \leq 50\text{Hz}$ noise on is just the right frequency that the neutrons pick up the first half of the period in the first part and the second half period in the second part of the spectrometer thus leading to a decreased apparent echo signal.

NSE is very sensitive to external magnetic perturbations as well as iron pieces displaced around the spectrometer during experiment.

In general the resolution is limited by magnetic field inhomogeneities. If one changes the collimation conditions, the the neutrons will explore different trajectories thus picking up different field inhomogeneities and the spectrometer resolution will change.

In summary , NSE spectroscopy is a ingenious way to combine high resolution with high counting rates. However when the resolution is pushed to its limits the number of important parameters which can give artifact increases rapidly. We tried to make an overview of those one we are aware of. In view of the limited number of

existing NSE spectrometers there might be others which are specific to each newly constructed one and extreme care in testing is highly recommended to make sure that artifacts are not at the origin of the observed effects.

References

- [1] Mezei, F. (editor) Neutron Spin Echo Lecture Notes in Physics 128 Springer-Verlag 1979
- [2] R. Gähler, R. Golub Z. Phys, B65 (1987) 269.



D.F.R. MILDNER

National Institute of Standards and Technology,
Gaithersburg, Maryland,
United States of America

Abstract

The principle of multiple mirror reflection from smooth surfaces at small grazing angles enables the transport and guiding of high intensity slow neutron beams to locations of low background for neutron scattering and absorption experiments and to provide facilities for multiple instruments. Curved guides have been widely used at cold neutron facilities to remove the unwanted radiation (fast neutrons and gamma rays) from the beam without the use of filters. A typical guide has transverse dimensions of 50 mm and, with a radius of curvature of 1 km, transmits wavelengths longer than 5 Å. Much tighter curves requires narrower transverse dimensions, otherwise there is little transmission. Typical neutron benders have a number of slots with transverse dimensions of ~5 mm. Based on the same principle but using a different technology, recent developments in glass polycapillary fibers have produced miniature versions of neutron guides. Fibers with many thousands of channels having sizes of ~10 μm enable beams of long wavelength neutrons ($\lambda > 4 \text{ \AA}$) to be transmitted efficiently in a radius of curvature as small as a fraction of 1 m. A large collection of these miniature versions of neutron guides can be used to bend the neutron trajectories such that the incident beam can be focused.

Neutron Lens Gain

The gain of a neutron focusing lens [1] using capillary optics depends upon three factors.

1) The proportion in angular space of those neutrons incident on the front face of the lens which may be transmitted by the lens is given by $(\theta_c/\theta_d)^2$, where θ_c is the critical angle of the glass composing the lens for some given wavelength, and θ_d is the divergence angle of the incident beam at the same wavelength. If the lens is placed at the exit at the exit of a neutron guide then θ_d is simply the critical angle of the guide at that wavelength. If $\theta_c > \theta_d$, then the factor is unity.

2) The area reduction of the beam is given by the ratio of the open area of the fibers and the size of the beam at the focus. This is given by $N\pi R^2 f_F / (\pi\sigma^2)$, where N is the number of fibers within the lens, R is the radius of the fibers, and f_F is the fractional open area of the fibers. The area of the focal spot is conveniently determined by the FWHM of the beam, that is, $\pi\sigma^2 = (\pi/2) (R^2 + L_F^2\theta_c^2)$, where L_F is the focal length of the lens, and θ_c is the critical angle of the glass averaged over the distribution of wavelengths transmitted by the focusing lens.

3) The transmission factor of a fiber depends on the radius of curvature ρ of the fiber and on the neutron wavelength, and decreases for smaller curvatures and therefore at increasing distances from the central straight fiber. The transmission also decreases for the curved capillaries for shorter wavelengths. This transmission function is complicated and for a parallel incident beam [2] is given by

$$T = \pi^{-1} \{ \pi - 2\psi - \sin 2\psi + 4\gamma \log[(1 + \tan(\psi/2))/(1 - \tan(\psi/2))] \} , \quad (1)$$

where $\cos\psi = \gamma^{1/3}$ and $\gamma = (\rho\theta_c^2/4R)$.

If I_0 is the beam current density of the beam incident on the entrance of the lens, the beam current density at the focus is given by

$$I_F = I_0 (\theta_c/\theta_d)^2 N\pi R^2 f_F T / (\pi\sigma^2) , \quad (2)$$

and therefore the gain G of the lens is given by

$$G = I_F / I_0 = (\theta_c/\theta_d)^2 N R^2 f_F T / (R^2 + L_F^2 \theta_c^2) . \quad (3)$$

Note that there is also a factor of 0.63 which reflects the fact that the focus does not have a uniform current density but rather a Gaussian distribution with a variance given by

$$\sigma^2 = (1/2) (R^2 + L_F^2 \theta_c^2). \quad (4)$$

Ignoring for the moment the transmission factor T , it is clear that the gain for a particular lens depends on the characteristics of the particular incident beam. Hence to quote a gain of the lens without reference to the incident beam is meaningless. Note that the gain is dependent on the incident divergence of the incident beam. If the incident beam is highly collimated such that $\theta_d > \theta_c$, the divergence factor $(\theta_c/\theta_d)^2$ is replaced by unity.

At infinite focal length ($L_F = \infty$), $T = 1$ for all fibers, but the focus is large and the gain is less than 1. As the focal length is decreased the area reduction factor increases, and the gain increases. At much smaller focal lengths the fibers become more curved, and the transmission factor T becomes more important as it decreases more from unity. At some point there is an optimum focal distance. This is given [3] by $L_F \theta_c \sim R$.

However there are limitations. If the focal length is so short and the available beam area at the entrance of the lens is large, it may be that the outer fibers have such a short radius of curvature that their transmission is zero and do not contribute to the focusing. Consequently all applications of focusing techniques must be carefully designed.

The gain of the lens depends on the wavelength as well as the divergence of the incident beam. Neglecting transmission losses, and the Gaussian nature of the spatial distribution of the neutron distribution at the focus, the gain is given [4] by

$$\begin{aligned} G &= (\theta_c/\theta_d)^2 N R^2 f_F / (R^2 + L_F^2 \theta_c^2) & \theta_d > \theta_c \\ &= N R^2 f_F / (R^2 + L_F^2 \theta_c^2) & \theta_d < \theta_c \end{aligned} \quad (5)$$

Hence the gain of the lens increases as λ increases for $\theta_d > \theta_c$, whereas the gain decreases as λ increases for $\theta_d < \theta_c$. However if the lens is placed at the end of a guide, (θ_c/θ_d) is independent of λ , and the gain decreases as a function of λ for all λ . Hence again this is another example that the gain of a lens is dependent on the incident beam definition.

Neutron Focusing Lens

Experimental neutron studies have been performed both on individual fibers [5] and on focusing elements [6]. These results compare well with computer simulation, and therefore have served as design guidelines for new installations. Two prototype neutron lenses [7,8] have also been characterized; these data have provided information for a new lens [9] designed specifically for use with a cold neutron prompt gamma activation analysis (PGAA) facility.

The dimensions of this lens assembly are 85 mm in height, 112 mm in width, and 160 mm in length. The entrance area of the lens, 50 x 45 mm², is fully illuminated by the beam leaving a ⁵⁸Ni-coated guide which views a cold neutron source through a cold beryllium filter. The angular acceptance for this arrangement is given by $(\theta_c/\theta_d)^2 = (1.1/2.04)^2 = 0.29$. It is the real space reduction which produces the gain of the lens. The fractional filled area of the lens, defined by the ratio of the area occupied by the $N = 1763$ polycapillary fibers to that of the entire entrance, is 0.175. Each lead silicate fiber is 125 mm in length, hexagonal in cross section with a radius R of 0.25 mm and has a hexagonal arrangement of 1657 hollow channels, each about 9 μ m in diameter. The fractional open area f_F of each fiber is about 0.5, and the reduced transmission of the curved channels and that caused by the limited angular acceptance results in average transmission efficiency of about 20%.

The lens produces a focus at a distance of $L_F = 52$ mm for an incident cold beam ($\lambda > 4$ Å using a beryllium filter) of average wavelength ~ 5 Å. Hence the computed radius of the beam at the focus is $(1/\sqrt{2})(R^2 + L_F^2\theta_c^2)^{1/2} = (1/\sqrt{2})((0.25)^2 + (52 \times 1.1 \times 10^{-3} \times 5)^2)^{1/2} = 0.27$ mm. In practice, we find experimentally that the profile of the beam at the focus is given by a Gaussian function with a FWHM of 0.53 mm. If we take this as the diameter of the focused beam, the focal area is 0.22 mm². The area illuminated at the entrance is given by $N(\pi R^2)f_F = 1763 \times \pi \times (0.25)^2 \times 0.5 = 173$ mm². Hence the area reduction is 785. Together with the angular acceptance of 0.29, the expected gain is 228, ignoring the transmission factor. Experimentally we find over the FWHM of the focused beam profile that the gain is 80, indicating a transmission loss of 35%. This transmission loss is averaged over all the fibers, and is unity for a single straight fiber and much less than one for the outer fibers. The average transmission is given by an integral of the transmission of the fibers as a function of radius over the area of the lens exit.

The achieved gain in neutron current density of 80 within the area of focal diameter 0.53 mm is reasonable because the area reduction of the beam is over 2000 times. Initial PGAA measurements [10,11] have demonstrated for certain isotopes an enhanced sensitivity of 60 and a gain in signal-to-noise of 7, resulting in the detection limit being increased by 20. In addition, submillimeter spatial resolution is now available for large samples for PGAA.

There is a shift in the wavelength distribution for a white beam transmitted by a focusing lens [12]. It is difficult to measure this shift in the transmitted spectrum. It has been used estimated using attenuators in the beam, before and after the lens. The attenuation coefficient increases with the lens compared to without the lens. Though the increase is comparable to the margin of error of the measurements, but it does

indicate the shift to longer wavelengths. This has an effect on the absorption techniques because $\sigma_a \propto \lambda$, and the effective gain in terms of the thermal beam equivalent is even greater than expected. This shift is caused by changes in the transmission of the outer fibers with a larger radius of radius of curvature and a reduction in the transmission of the shorter wavelengths.

Experimental Considerations

The present lens focuses only a few percent of the neutrons incident on the entrance of the lens, determined from the fractional open area and the average transmission efficiency, so most of the neutrons which are incident on the entrance of the lens are not transmitted. Some strike the entrance of the lens in the spaces between fibers, others strike the fiber but are outside the open channels of the fibers, and others enter a channel but the grazing angle with the channel wall is above the critical angle. In practice, only a few percent of the neutrons which are incident upon the lens entrance are transmitted to the focus. This means that there is potential for high background problems.

Some of these neutrons are absorbed by the glass or other materials within the lens, to give rise to high prompt gamma background which may be deleterious, particularly to gamma ray measurements using the focused beam. Others are scattered by the materials of the lens and enter shielding materials and produce gammas. Others are not transmitted to the focus by the lens, but penetrate through the lens and provide a low intensity neutron beam around the focus which detracts from measurements on small areas of large samples, and thereby diminish the spatial resolution. All these occurrences require careful attention to shielding, both within the lens itself and around the sample under investigation and the detecting equipment.

The principle for focusing the neutrons makes necessary that the focused beam has a large divergence. This is defined by the outermost fibers of the lens, which in the above lens have a maximum bending angle (or half convergence angle) of about 13° . This is deleterious for neutron diffraction experiments, but is unimportant for neutron absorption measurements. Consequently a lens of this type is useful for absorption techniques such as PGAA and neutron depth profiling (NDP). In addition this angular convergence gives a sharp depth of focus.

The variance $\sigma^2(\ell)$ of the transverse distribution of neutrons in the focused beam as a function of the distance ℓ from the focal point may be written [1] as

$$\sigma^2(\ell) = 1/2 [\ell^2 \tan^2\Omega + R^2 + (L_F + \ell)^2 \theta_c^2], \quad (6)$$

where L_F is the focal length of the lens, R is the radius of the individual fibers, θ_c is the critical angle of the glass of the capillaries, and Ω is the convergence angle of the lens. That is, the angular convergence causes the beam area to decrease in diameter as a function of distance from the lens exit. It reaches a minimum at the focus and then diverges.

It is important that the sample is positioned accurately at the focal plane of the lens in order to take full advantage of the increase current density and spatial resolution of the focused beam. This is true for both lateral and transverse directions. For NDP the

focus should be placed at the front (or back) surface of the sample, since a depth of typically 1 or 2 μm is analyzed, depending whether the charged particle detector is viewing the front (or back) surface. On the other hand for PGAA measurements the entire thickness is analyzed, and it seems reasonable to place the disc sample such that the focus lies at the center of the disc width to minimize the volume analyzed. The transverse distribution of the intensity at the focus is so sharp (a Gaussian function with a FWHM ~ 0.53 mm for our lens) that it is important that a small area of interest is placed exactly at the focus, otherwise large errors will occur and any quantitative measurements will be flawed. The differences in the analysis of absorption measurements taken with a collimated (approximately parallel) beam and a focused beam using a converging lens have been considered [13].

Applications of Focused Beams

Initial tests [10,11] have been performed with the focusing lens for prompt gamma activation analysis (PGAA). These results indicate that two dimensional composition mapping will be available by scanning or rastering a large sample area through the neutron beam. The focusing technique will be applied to neutron depth profiling (NDP), and appears to be promising also for scanning purposes. However the application may be limited to large flux sources, because the total number of neutrons is very limited at lower source strengths.

This focusing concept will ultimately be used for the development of a real-time neutron imaging probe for compositional studies, which might incorporate either PGAA (producing two dimensional imaging of objects) or NDP (producing three dimensional mapping of the surface of certain objects). A bender-focuser lens [14] can enable the focal spot to be placed outside the shadow of the incident beam and therefore in an area of lower background. A bender can also be used to create a pseudo end-guide position which is highly desirable for low background measurements. Various ideas have been proposed for the use of a neutron focusing lens in different branches of physics.

Small-angle neutron scattering generally uses large source and sample areas with long flight paths to obtain the necessary resolution. Increased count rates may be obtained using collimators that converge to a point on the detector. Further increases may be obtained by converging guides in the form of a focusing lens. However such a technique using converging capillary fibers produces only a low resolution instrument requiring the use of a detector that has fine spatial resolution, perhaps less than 0.1 mm. Expressions [15] have been given for the resolution and the intensity optimized for such an instrument. The relationship is determined between the guide dimensions, the focal length and the critical angle of the internal coating of the individual fibers. The latter dominates the resolution, such that the instrument is useful only for low resolution measurements. However the size of the instrument is greatly reduced (from perhaps tens of meters to about 0.5 m), so that despite its low resolution, such an instrument could be useful for survey or characterization measurements. An initial test [16] of this concept has been undertaken using a prototype focusing lens, in conjunction with a video radiation detector which has an efficiency of only a few percent. However neutron imaging plate detectors have a much higher efficiency and should be able to prove the technique. The polycapillary focusing technique with a neutron imaging plate detector can also be used for radiography.

A focusing lens can also be used in nuclear physics experiments, for example for the measurement of the neutron capture cross section of the isomeric state of ^{178}Hf and its capture gamma-ray spectrum [17]. This metastable isotope (half-life of 31 years) may now be produced in sufficient quantities that it can be used as a high-spin target ($I^\pi = 16^+$) for nuclear structure and nuclear reaction studies. However it is expensive to produce even reasonable quantities of the metastable isotope, and these gamma ray coincidence measurements are difficult even with the greatest flux because the amount of the sample is small. Again since this is an absorption measurement the use of a focusing lens is beneficial for increasing the available flux on the very small specimen.

Finally, neutron capillary optics can contribute significantly to important boron neutron capture therapy (BNCT) for cancer [18]. Although most BNCT efforts now use epithermal neutrons because their penetrating power is superior to thermal neutrons, cancer research on small animals can use slow neutron beams free of fast neutrons and gamma rays. An example is the study of the radiobiological effects of neutron capture reactions on normal tissues and transplanted brain tumors in rodents for different boronated compounds. In addition, neutron capillary optics can provide a sensitive method for non-invasive neutron imaging of ^{10}B distribution in small living animals, useful for the development of tumor-selective boron compounds.

Discussion

At the present the use of polycapillary optics may have limited use for the enhancement of the utilization of low and medium flux research reactors. It is clear that this new concept improves the capabilities of neutron absorption techniques such as PGAA, NDP and radiography. However the consideration of using capillary optics should only be taken if these techniques are already in use at the facility, so that the concept can be fully exploited. The various other ideas that have been outlined look promising enough, but it may take a few years before all the various teething problems are adequately addressed.

Capillary optics work best with cold (long wavelength) neutrons because the critical angle (and there the acceptance solid angle) increases with wavelength. This would suggest that these focusing lenses can only be placed at reactor facilities which have a cold source. Certainly there are most advantageous at cold neutron facilities. However, a focusing lens using capillary optics can be used with thermal beams. The average critical angle θ_c will be lower, and the most highly curved fibers will have zero transmission. Hence the gains will not be as high as for cold neutron beams, but the lens can be designed such that it can be of benefit.

It is always useful to increasing the real space acceptance of the lens. However this is likely to increase the length of the lens, and consequently increase the number of reflections and the transmission losses. In addition the transmission of an S curve has a complete cut-off at short wavelengths, so that a reduced transmission is likely to result in a reduced gain. However a polycapillary fiber bender-focuser [18] has been designed, which takes the focus to a region of lower background outside the shadow of the incident beam. It remains to be seen whether the expectation that the reduction in signal is more than offset by the considerable reduction in background.

The best idea for increasing the acceptance area is the concept of tapered capillary channels. This is a refinement on the polycapillary fiber lens. A large number of fibers are fused together and drawn so that the entrance area does not have any open space, and at the exit all the channels directed to the common focus. This results in two improvements. The acceptance area is more concentrated, so that fewer incident neutrons are wasted and give rise to background, and individual channels, rather than individual fibers are directed to the focus, so that smaller focal spots are expected.

This idea has been tested with cold neutrons with promising results [19]. A monolithic lens consisting of a fused tapered bundle of polycapillaries has been shown to provide a smaller focus of about 0.16 mm, and gains comparable with polycapillary lenses. The cross section of these monolithic devices is much smaller than for polycapillary lenses, so at present their application is limited. This concept will be used in the NDP facility which has a more compact volume, and will enable the three dimensional mapping of the surface of thin-film semiconductor materials, for example. However their further development may enable greater gains than have already been achieved with the polycapillary lenses. Ultimately, the lens concept using tapered capillaries has the potential for use as part of a neutron microscope with a spot size of less than 0.1 mm.

Only if the focusing lens has some monochromatization device, such as being placed after a monochromator crystal, can the lens can be used for inelastic neutron scattering experiments where good Q resolution is not required with polycrystalline sample of small size. However, with the present technology a focusing lens in conjunction with a monochromator is unable to give greater current density gains than the focusing available with curved perfect monochromators. In addition, the intensity gain at the cost of beam collimation makes the focusing lens unlikely to be useful as a device for neutron scattering techniques that require good Q resolution.

Possible low-resolution small-angle neutron scattering measurements with a focusing lens has yet to be proved. However ingenious the idea may be, its applications may be limited to scanning purposes where only intensity on small regions is important. The intensity in the wings (sometimes called 'halo') around the direct beam prevents usual SANS measurements, but some applications may be found with very strong scatterers. It is important that high spatial resolution ($\sim 10 \mu\text{m}$) on the detector such as provided by imaging plate detectors is necessary for SANS using a polycapillary lens in order to match the resolution conditions.

Two rather far-fetched ideas, for which the technology does not exist currently, may one day be realized. One is the coating of the inside of the capillaries with a metal such as nickel to increase the critical angle per unit wavelength. This would allow for greater transmission for curved fibers and increase the available gains in neutron current density, though the size of the focal spot will not be slightly larger. The other is a variable focusing device that might allow variations in studies of materials as a function of depth. Such a development might lend itself to a neutron microprobe.

Polarization analysis / depolarization studies may exploit the divergence of a capillary lens by using a polarizing ^3He spin filter before the lens to obtain a highly focused polarized beam to fall on the sample. The transmitted beam with a large divergence can be analyzed fully by another polarizing ^3He filter. This technique enables the

ability to scan a given sample and obtain spatial information on a fine scale, for example, domain structures sizes, etc. At present the polarizing ^3He filter is still in the development stage. The current best results have a transmission of about 32% with a polarization of about 85%. However the technique looks promising for the future.

Numerous discussions with colleagues at NIST and at X-Ray Optical Systems, Inc., are acknowledged, in particular Heather Chen-Mayer, Greg Downing, Qi-fan Xiao and Vasily Sharov.

REFERENCES

1. D.F.R. Mildner and H. Chen, *J. Appl. Cryst.* **27**, 943-949 (1994).
2. M.A. Kumakhov and F.F. Komarov, *Phys. Rep.*, **191** 289-350 (1990).
3. D.F.R. Mildner, *J. Appl. Cryst.*, **26**, 721-727 (1993).
4. D.F.R. Mildner, H. Chen, V.A. Sharov, R.G. Downing and Q.F. Xiao, *Physica B* **213&214**, 966-968 (1995).
5. H. Chen, D.F.R. Mildner, R.G. Downing, R.E. Benenson, Q.F. Xiao and V.A. Sharov, *Nucl. Instrum. Meth.* **B89**, 401-411 (1994).
6. Q.F. Xiao, H. Chen, D.F.R. Mildner, R.G. Downing and R.E. Benenson, *Rev. Sci. Instrum.* **64**, 3252-3257 (1993).
7. H. Chen, R.G. Downing, D.F.R. Mildner and V.A. Sharov, in *Neutron Optical Devices and Applications* (eds., C.F. Majkrzak and J.L. Wood), SPIE conference, San Diego, July 1992, **1738**, 395-404 (1992).
8. H. Chen, D.F.R. Mildner and Q.F. Xiao, *Appl. Phys. Lett.* **64**, 2068-2070 (1994).
9. Q.F. Xiao, H. Chen, V.A. Sharov, D.F.R. Mildner, R.G. Downing, N. Gao and D.M. Gibson, *Rev. Sci. Instrum.* **65**, 3399-3402 (1994).
10. H. Chen, V.A. Sharov, D.F.R. Mildner, R.G. Downing, R.L. Paul, R.M. Lindstrom, C.J. Zeissler and Q.F. Xiao, *Nucl. Instrum. & Meth.* **B95**, 107-114 (1995).
11. H.H. Chen-Mayer, V.A. Sharov, D.F.R. Mildner, R.G. Downing, R.L. Paul, R.M. Lindstrom, C.J. Zeissler and Q.F. Xiao, *J. Radioanal. Nucl. Chem.*, in press (1996).
12. D.F.R. Mildner, H. Chen, R.G. Downing, V.A. Sharov and Q.F. Xiao, *Acta Physica Hungarica* **75**, 177-183 (1994).
13. D.F.R. Mildner, H.H. Chen-Mayer and R.G. Downing, *Proc. Intl. Symp. Neutron Optics*, March 1996, Kumatori, Japan, *J. Phys. Soc. Japan*, in press (1997).
14. Q.F. Xiao, V.A. Sharov, R.G. Downing, H.H. Chen-Mayer and D.F.R. Mildner, *Proc. Intl. Symp. Neutron Optics*, March 1996, Kumatori, Japan, *J. Phys. Soc. Japan*, in press (1997).
15. D.F.R. Mildner, *J. Appl. Cryst.* **27**, 521-526 (1994).
16. D.F.R. Mildner, H. Chen, R.G. Downing, R.E. Benenson and C.J. Glinka, *J. de Phys.* **IV**, Coll. **C8**, **3**, 435-438 (1993).
17. H. Börner, private communication (1995).
18. Q.F. Xiao, V.A. Sharov, D.M. Gibson, H. Chen, D.F.R. Mildner and R.G. Downing, *Proc. 6th Intl. Symp. Neutron Capture Therapy for Cancer*, October 1994, Kobe, Japan. *Cancer Neutron Capture Therapy* (ed. Y. Mishima) Plenum Press, New York, 399-406 (1996).
19. H.H. Chen-Mayer, D.F.R. Mildner, V.A. Sharov, J.B. Ullrich, I. Yu. Ponomarev and R.G. Downing, *Proc. Intl. Symp. Neutron Optics*, March 1996, Kumatori, Japan, *J. Phys. Soc. Japan*, in press (1997).

LIST OF PARTICIPANTS

- Akhtar, K. Division of Physical and Chemical Sciences,
International Atomic Energy Agency,
P.O. Box 100, A-1400 Vienna, Austria
- Clausen, K.N. Risø National Laboratory,
Department of Solid State Physics,
P.O. Box 49,
DK-4000 Roskilde, Denmark
phone: 45-46-77-4704; fax: 45-42-37-0115; E-mail: clausen@risoe.dk
- Farago, B. Institute Max van Laue-Paul Langevin,
B.P. 156,
F-38042 Grenoble Cedex 9, France
phone: 33-76-20-7347; fax: 33-76-48-3906; E-mail: farago@ill.fr
- Goyal, P.S. Solid State Physics Division,
Bhabha Atomic Research Centre,
Bombay-400085, India
phone:022-5563060 Ext. 4236; fax: 022-5560750;
E-mail: psgoyal@magnum.barc.ernet.in
- Mildner, D. National Institute of Standards and Technology,
Nuclear Methods Group,
Analytical Chemistry Division,
Gaithersburg, MD 20899, USA
phone: 1-301-975-6366; fax: 1-301-208-9279;
E-mail: mildner@enh.nist.gov
- Rekvelde, M.T. Interfacultair Reactor Instituut,
Technische Universiteit Delft,
Mekelweg 15,
NL-2629 JB Delft, Netherlands
phone:31-15-782107; fax: 31-15-786422